MULLARD LIMITED
Mullard House
Torrington Place
London, W.C.1

CONTENTS

Ferrite-cored Inductors and Transformers	30-42
Performance of AAY39 Mixer Diode with Narrow Band T-R Cell	43-45
Idealised Rectifier Circuit Performances	46-47
Firing of Ignitrons by means of Thyristors	48-52

VOL. 9 No. 82 JULY 1966

Mullard Technical Communications

VOLUME 9 NUMBER 82 July 1966

Mullard Technical Communications

VOLUME 9 NUMBER 82 July 1966

Contents

Ferrite-cored Inductors and Transformers *E. C. Snelling* 30

Performance of AAY39 Mixer Diode with Narrow Band T-R Cell *T. H. Oxley and R. W. Yell* 43

Idealised Rectifier Circuit Performances 46

Firing of Ignitrons by means of Thyristors *H. J. G. M. van Daelen* 48

Mullard Technical Communications contains information on the performance or application of Mullard products such as semiconductor devices, electronic valves and tubes, and electrical and magnetic components. It is issued free-of-charge to equipment designers, research organisations, reference libraries, and educational establishments. Bona fide applications to be added to the circulation list should be made under an official letter head to Central Technical Services. Overseas enquiries should be addressed to the local Mullard agent, or to Mullard Export Division at Mullard House.

Abstracts, or references to an article, should mention both the source, *Mullard Technical Communications*, and the authors. Requests for republication or translation should be made to the Editor in writing.

The issue of the information contained in this publication does not imply any authority or licence for the utilisation of any patented feature.

'Mullard' is the trade mark of Mullard Limited and is registered in most of the principal countries of the world.

Editor: F. A. Sowan
Assistant Editor: E. G. Evans

Published by
Central Technical Services
Mullard Limited, Mullard House, Torrington Place, London, W.C.1
LANgham 6633

© Mullard Limited, 1966

Made and Printed in England by
WIGHTMAN AND COMPANY LIMITED, 1/3 BRIXTON ROAD, LONDON, S.W.9

Ferrite-cored Inductors and Transformers

E. C. Snelling
Mullard Research Laboratories

This article is in two parts. The first part describes the history of the use of ferrites in inductor cores, and discusses the inductance, Q, and losses of such inductors. The second part describes the use of ferrites in transformer cores with particular reference to wide-band medium frequency transformers, wide-band r.f. transformers, low power pulse transformers and high frequency high power transformers.

GENERAL INTRODUCTION

Ferrites have been in use for the cores of inductive components since the introduction of ferrites in about 1948. Different types of ferrites and a great variety of core shapes, however, have been developed to meet the demands of different kinds of applications. The present article is divided into two parts, the first dealing with inductor cores, the second with transformer cores.

In the part concerning inductor cores, a brief history of the ferrites is followed by a discussion of the inductance, Q and losses of a typical ferrite inductor core.

In the part concerning transformer cores, the general transformer theory is followed by a comparison of ferrite and ferromagnetic transformer cores, and by a description of four particular kinds of transformers. These are wide-band medium frequency communications transformers, wide-band r.f. transformers, low power pulse transformers, and high frequency high power transformers.

Part 1—Ferrite-cored Inductors

INTRODUCTION

High quality inductors are used in very large quantities in carrier telephony circuits as elements in filters and equalisers. Even larger numbers of inductors are used in the less exacting selective circuits of entertainment electronics and in a wide range of industrial electronics. In this article only the telephony application will be considered as it embraces most of the problems and techniques.

In the early days, telephony inductors used powder-iron toroidal cores, first at low frequencies and then, as carrier telephony transmission developed, at higher frequencies. At carrier frequencies the core losses were relatively high and this led to bulky designs to achieve the required quality. Improvements were made as nickel iron powdered cores with lower losses became available. Eddy current losses in the metallic particles continued to limit the performance. About 1946 ferrites were introduced (Ref. 1) specifically for this application. Having resistivities about 10^6 times greater than the metals, they could be made as solid cores with almost negligible eddy current core loss. They could be used in the form of cylindrical cores enclosing an annular winding. Because the intrinsic permeabilities of the cores were high, the coupling caused by stray magnetic fields was negligible; the reverse was true of powder cores and it prevented their use in this compact form. As ferrite technology developed, core shapes and properties improved and the overall size decreased. Fig. 1 illustrates the progress.

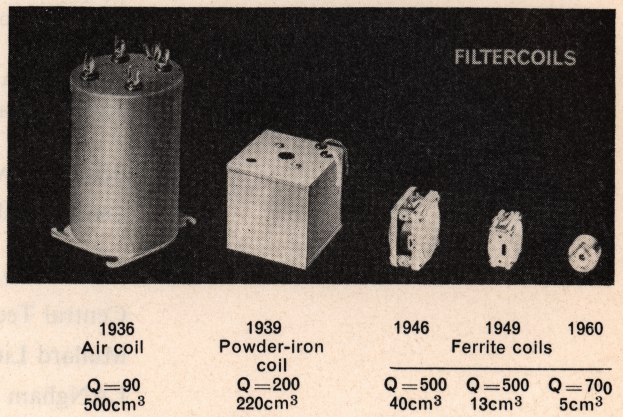

Fig. 1—Historical development of inductors for telecommunications

The cylindrical construction, known as a pot core, is shown in Fig. 2. Originally the core was formed by a concentric cylinder and ring sandwiched between two circular plates. It is well known that the best overall performance may be obtained if an air gap of the correct length is introduced into the core (Ref. 2). This was done by making the central member somewhat shorter; inductance adjustment was achieved by grinding this member until the correct inductance was obtained. Later, the construction was simplified into two core halves as shown in Fig. 2. The mating surfaces are ground flat to provide a stable, low-reluctance contact. The air gap is now in the centre and inductance adjustment may be achieved by varying the position of a ferrite cylinder which shunts the gap. There are various ways in which this may be done; in the version illustrated a ferrite tube is attached to a plastic carrier which is screwed up or down on a threaded stud (Ref. 6).

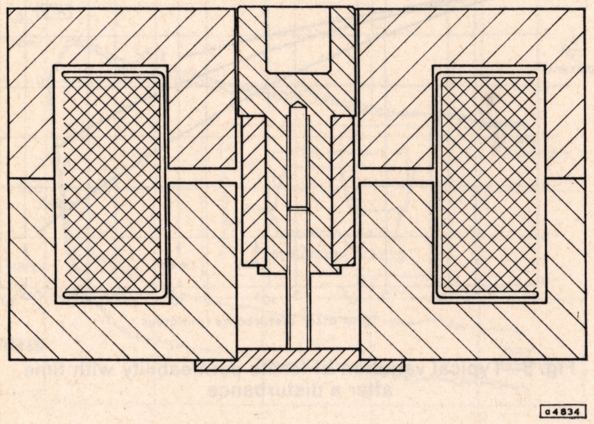

Fig. 2—Cross-section of a typical pot core

The dimensional proportions of the core obviously influence the performance. If the winding space is very small, very fine wire is necessary to achieve a given inductance, so the loss due to winding resistance is high. Alternatively, if the winding space is relatively very large there would be very little core material and many turns of fine wire are necessary to obtain a given inductance; again the winding loss is high. Somewhere between these extremes, there is an optimum. The optimum proportions were calculated at our Laboratories (Ref. 2) in 1957 and with small variations they are used in the ferrite pot cores currently available. The present practice is for pot cores to be available in a range of sizes. They have substantially the same proportions as each other and have similar design features. Fig. 3 shows some typical examples.

In addition to having the optimum size and shape, the ferrite core must have the most suitable magnetic properties. The manufacturer controls parameters such as the permeability of the ferrite, the effective permeability of the gapped core, the magnetic losses, the temperature dependence of the permeability, the time stability of the permeability, and the material resistivity (Ref. 2). An inductor, however, is more than a pair of ferrite half-cores. It requires a winding, a means of adjustment and a technique of assembly. These contributions influence the inductor performance at least as much as the ferrite parts and because they are not under direct control of the ferrite manufacturer they give rise to most of the design problems.

It can be said that the filter manufacturer requires an element that, ideally, is an inductance, a constant inductance, and nothing but an inductance. In other words, the inductor should have very low losses, and once it has been adjusted to its required value of inductance it should remain constant during the life of the filter. There are other requirements such as adequate adjustment range, low waveform distortion and low overall cost and volume, but the major considerations in present day inductor technology are low loss and the greatest constancy of inductance; it is to these aspects that the remainder of this part of the article is devoted.

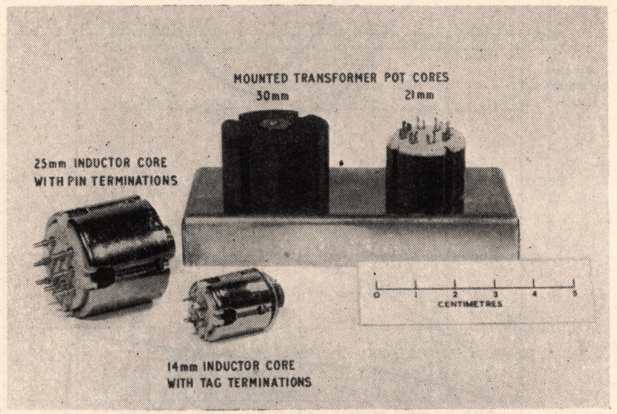

Fig. 3—Typical pot core assemblies

INDUCTANCE CONSTANCY

In most of the critical circuits the filter designer is ultimately concerned with the constancy of resonant frequencies, or in terms of elements, the constancy of LC products. The inductance and capacitance will both vary reversibly with temperature; that is, they will have temperature coefficients. In general, they will also vary with time under the influence of environmental conditions; that is, there will be irreversible changes.

The temperature coefficient (T.C.) of the capacitor depends mainly on the dielectric, and there is little room for manoeuvre. Given a type of capacitor, the nominal T.C. is fixed and the tolerance on the T.C. is a matter of cost. The ferrite is somewhat more accommodating, at least over a limited temperature range, and it is possible to attempt some compensation by arranging that the nominal value of the inductor T.C. is equal and opposite to that of the capacitor. In any case the tolerance on the T.C. of the LC product equals the sum of the component T.C. tolerances. Compensation is usually attempted when polystyrene foil capacitors are used; they have nominal

---

This article is based directly on the texts of two lectures given by the author in March 1966 at a Symposium on the Electrical Engineering aspects of Ferrites, held at Woolwich Polytechnic.

T.C. values of about -130×10^{-6} per degC. If the inductor nominal T.C. value is exactly equal and opposite to this then it follows that the maximum T.C. of the LC product will equal half the sum of the component T.C. tolerances. Thus it is important to minimise the T.C. tolerance. Fig. 4 shows some typical permeability versus temperature curves. The slope of the basic curve is often too great for useful compensation, but by introducing a 'hump' in the region of 0°C it is possible to adjust the slope over the normal operating temperature range. The A13 curve illustrates this to a marked degree. Provided a reasonable positive T.C. is required, the manufacturing tolerance depends mainly on economics. Zero or negative T.C. values (to match, for example, silvered mica capacitors) are more difficult. Over a limited temperature range they may be obtained by enhancing the effect of the hump, but the curve becomes S-shaped and a region having an average T.C. of zero will include both positive and negative slopes. The required tolerances then become more difficult to hold.

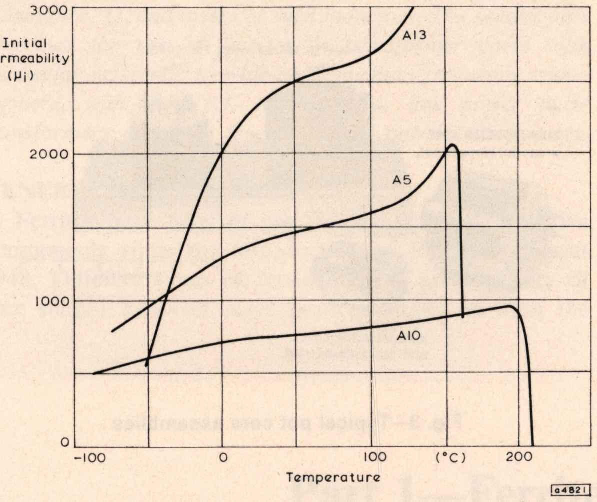

Fig. 4—Permeability shown as a function of temperature for three typical ferrite materials

Over a limited temperature range the T.C. of the ferrite material is given by

$$(\text{T.C.}) = \frac{\Delta\mu}{\mu\Delta T}. \qquad \ldots(1)$$

When a ferrite material is used in a core which has an air gap, such that it appears to have an effective permeability μ_e, then the T.C. of the gapped core is given by

$$(\text{T.C.})_{\text{gapped}} = (\text{T.C.}).\frac{\mu_e}{\mu}$$

$$= \frac{\Delta\mu}{\mu^2\Delta T}.\mu_e \qquad \ldots(2)$$

$$= (\text{T.F.}).\mu_e \qquad \ldots(3)$$

where T.F. is the temperature factor, or normalised material temperature coefficient. This is the parameter controlled by the ferrite manufacturer. If T.F. $= 1{\cdot}0 \times 10^{-6}$ per degC then, for a core having $\mu_e = 100$, the temperature coefficient would be 100×10^{-6} per degC.

This approach is limited to relatively small temperature ranges; over larger ranges, where the curvature of the permeability versus temperature relationship is significant, the specification must be more functional and graphical boundaries are sometimes used.

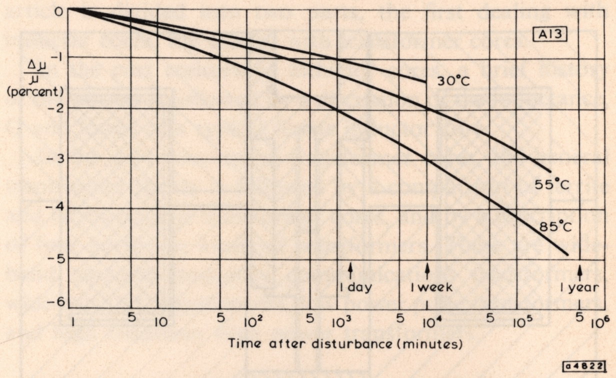

Fig. 5—Typical variation of ferrite permeability with time after a disturbance

In addition to the reversible effects, there are irreversible effects. The capacitance and inductance values will in general drift during life. Considering only the inductor, obviously any time change of permeability will cause drift. This has been discussed at length in the literature (Refs. 2 and 3). Briefly, if a ferrite (or, in fact, any magnetic material) is given a magnetic, thermal or mechanical disturbance, the permeability will immediately rise above the stable value, to which it will subsequently return as a function of time. This process is repeatable and thus differs from chemical ageing, a phenomenon which is virtually absent in ferrites. Fig. 5 shows the time change of permeability following a magnetic shock (an a.c. field diminishing from saturation). The change depends on the temperature; at room temperature a change of 1% between 1 minute and 24 hours after the disturbance is typical. The phenomenon is called disaccommodation and it is expressed by a disaccommodation factor (D.F.) where

$$(\text{D.F.}) = \frac{\Delta\mu}{\mu^2} \qquad \ldots(4)$$

and where the times must be specified. (Ref. 2).

So far only the ferrite contributions have been considered. Usually the winding, the adjuster and the assembly technique will all contribute both reversibly and irreversibly. The reversible contributions will modify the T.C. For example, in a poorly designed adjuster, the position of the magnetic shunt will be significantly influenced by the linear expansion of the support members. In addition, the clamping pressure, or the winding geometry, may vary with temperature and significantly affect the inductance. Any contribution from the non-ferrite parts will cause the T.C. of the inductor to depart from the value given by $(\text{T.F.}).\mu_e$. Since, as stated above, the tolerance on the overall T.C. is important, such uncertain contributions are to be avoided.

Even more important are the irreversible contributions from the non-ferrite parts. These will cause the inductance to drift during the service life. There are many possible contributions, and it requires sustained investigations of high resolution to identify them. One technique is to subject a carefully prepared batch of inductors to a number of precisely controlled dry temperature cycles. It is assumed that the temperature cycling accelerates the action of the drift mechanisms. The inductors are allowed to acclimatise for an adequate period at the upper and lower temperature of each cycle. The inductance is measured at a suitable point in each cycle (for example, just before the temperature is raised), and a graph is plotted showing the variation of this inductance with number of cycles.

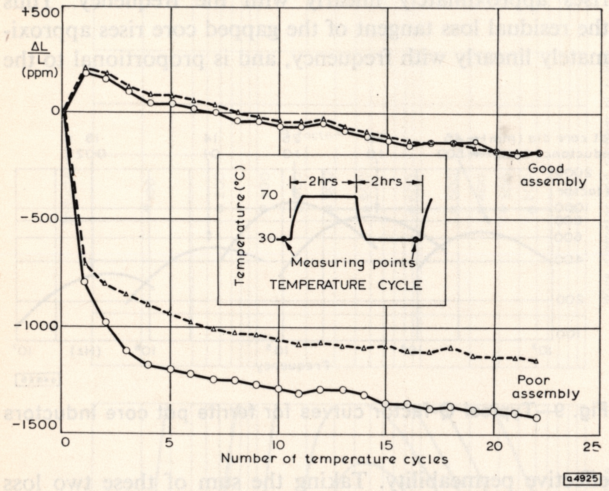

Fig. 6—Drift of inductance of cemented pot cores

Fig. 6 shows some typical results of such an investigation. It is seen that a poor assembly may give an inductance drift of as much as 0·1% during the first few cycles and it may continue to drift for many cycles. A good assembly would not drift excessively during the initial few cycles and would reach a stable value that is within a few 100 ppm of the starting value. In both cases the drift is mainly caused by non-ferrite parts. The contribution from disaccommodation is largely eliminated by the regular nature of the cycle, except for the first cycle where a small inductance rise might be expected; the upper curve shows such a rise. The main contribution in the examples illustrated is the creep of the joint between the two half pot cores. It is usual to cement this joint with epoxy resin and there is a small progressive change of joint thickness after the joint has been cured. This is accelerated by increase of temperature.

If any part of the construction is stressed by, for example, thermal effects during assembly, or by the pressure of a spring clamp, then stress relief is to be expected during life and this also will be accelerated by temperature cycling.

Comparable with the contribution from the cemented joint is that from the adjuster. This must be able to provide perhaps a ±10% adjustment of inductance and thereafter have negligible residual effect on the inductance. Fig. 7 shows typical adjustment curves. To achieve adequate setting accuracy the screw thread should have a fine pitch, with a smooth action that gives no backlash. If the adjustment curve is to be reproducible, and free of waviness, the dimensional and form tolerances of the adjusting mechanism must be made small. In addition to these adjuster requirements, the design must be such that the adjuster is in a substantially stress-free condition at the end of the adjustment process. If it is not, then the adjuster may cause appreciable inductance drift. Fig. 8 shows a comparison between the performance of an adjuster in which no special attention has been paid to stability and the performance that is possible with care in design. In both cases the contributions of other effects have been eliminated.

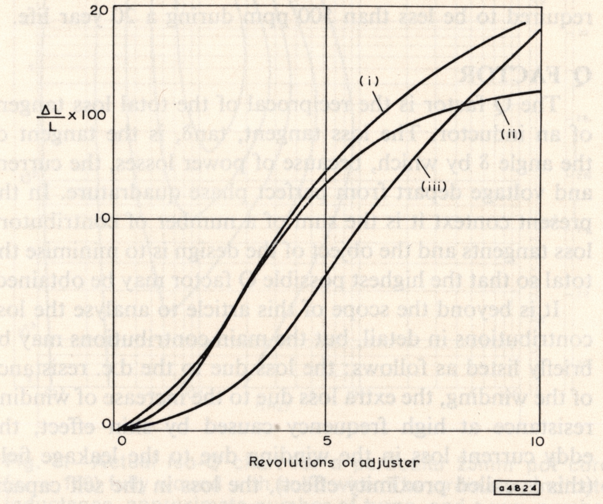

Fig. 7—Typical adjustment curves for pot cores
Core (i) has diameter 18mm and μ_e 160
Core (ii) has diameter 25mm and μ_e 40
Core (iii) has diameter 35mm and μ_e 100

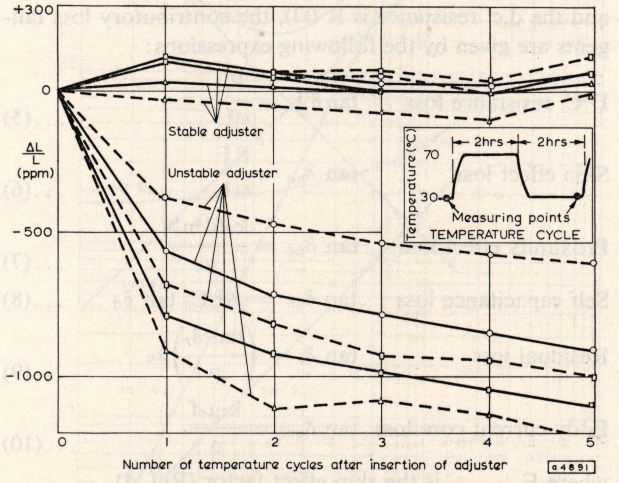

Fig. 8—Variability of inductance caused by movement of the adjuster during temperature cycling

Other environmental conditions, such as humidity and vibration, will cause inductance drift, but these do not play such an important part in the service life of a telephony inductor and it is for this application that extreme stability is required.

Finally, it is useful to state figures which are typical of the more severe present day requirements. The T.C. of inductance may be required to be within ±40 ppm per degC of a specified nominal; the inductance drift is often required to be less than 500 ppm during a 20 year life.

Q FACTOR

The Q factor is the reciprocal of the total loss tangent of an inductor. The loss tangent, tanδ, is the tangent of the angle δ by which, because of power losses, the current and voltage depart from perfect phase quadrature. In the present context it is the sum of a number of contributory loss tangents and the object of the design is to minimise the total so that the highest possible Q factor may be obtained.

It is beyond the scope of this article to analyse the loss contributions in detail, but the main contributions may be briefly listed as follows: the loss due to the d.c. resistance of the winding, the extra loss due to the increase of winding resistance at high frequency caused by skin effect, the eddy current loss in the winding due to the leakage field (this is called proximity effect), the loss in the self capacitance, the residual loss in the ferrite core and the eddy current loss in the ferrite core.

For a ferrite pot core inductor operating at an angular frequency $\omega = 2\pi f$, having an effective permeability μ_e, and wound with N turns such that the inductance is L (H) and the d.c. resistance is R (Ω), the contributory loss tangents are given by the following expressions:

D.C. resistance loss
$$\tan\delta_{dc} = \frac{R}{\omega L} \qquad \ldots(5)$$

Skin effect loss
$$\tan\delta_{se} = \frac{RF}{\omega L} \qquad \ldots(6)$$

Proximity effect loss
$$\tan\delta_{pe} = \frac{k_e f d^4 n N}{\mu_e} \qquad \ldots(7)$$

Self capacitance loss
$$\tan\delta_{sc} = \omega^2 L C_s \tan\delta_d \qquad \ldots(8)$$

Residual loss
$$\tan\delta_r = \left(\frac{\tan\delta_r}{\mu}\right)\mu_e \qquad \ldots(9)$$

Eddy current core loss
$$\tan\delta_{ecf} = \frac{k_f \mu_e f}{\rho}, \qquad \ldots(10)$$

where F is the skin effect factor (Ref. 4),

k_e is a proximity effect constant characterising a particular pot core,

d is the copper diameter of the wire if solid, or the strand if bunched conductors are used,

n is the number of strands in the case of bunched conductors; (n = 1 for solid wire),

C_s is the self capacitance,

$\tan\delta_d$ is the dielectric loss tangent of the self capacitance,

$\left(\frac{\tan\delta_r}{\mu}\right)$ is the residual core loss factor of the ferrite material,

k_f is the eddy current core constant,

ρ is the core resistivity.

Hysteresis loss in the core has been omitted from this list because telephony inductors usually operate at such low amplitudes that the hysteresis loss is negligible. The loss components are considered in more detail in Refs. 5 and 6.

All the loss tangents are functions of μ_e and f. Consider, for example, $\tan\delta_{dc}$. This is inversely proportional to μ_e and f (because $L \propto \mu_e$) and it is a major loss contribution. Another major loss is the ferrite core loss. This is characterised by a material parameter called the residual loss factor $\left(\frac{\tan\delta_r}{\mu}\right)$, which, over a wide frequency range, rises approximately linearly with the frequency. Thus the residual loss tangent of the gapped core rises approximately linearly with frequency, and is proportional to the effective permeability. Taking the sum of these two loss tangents alone, the total loss tangent $\tan\delta_{tot}$ can be expressed approximately as follows.

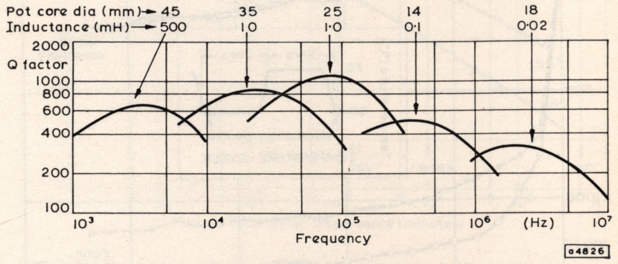

Fig. 9—Typical Q-factor curves for ferrite pot core inductors

$$\tan\delta_{tot} \simeq \frac{A}{f\,\mu_e} + (B + Cf)\,\mu_e \qquad \ldots\ldots(11)$$

where A, B and C are constants for a given pot core.

This will clearly have a minimum; for a given value of μ_e this will occur at a particular frequency, or for a given frequency it will be obtained with a particular value of μ_e. In practice all the possible loss tangents must be taken into account and the total loss tangent will depend on all aspects of the design. Fig. 9 shows some typical Q factors as functions of frequency; an increase in effective permeability moves the peaks to lower frequencies.

Originally it was usual to describe the performance of pot cores in terms of a few Q curves obtained by measurement. More recently, extensive study of the nature of the contributory loss tangents, particularly the eddy current loss contributions, has led to the possibility of reliable calculation. This has a great advantage over measurement. In calculation, the starting data may be carefully chosen to represent the average values likely to be encountered in practice. Because of manufacturing tolerances measurement is subject to randomness that can only be eliminated by using a very large number of samples.

Individual Q curves are not very helpful unless they happen to coincide with a particular requirement; since they depend on, among other things, the inductance and the type of wire, such coincidence is unlikely. However, if the curves can be computed, then they may be obtained systematically over the appropriate range of each of the major variables. The results may be presented as iso-Q charts with inductance and frequency as coordinates. The construction of such a chart is shown in Fig. 10. For a given pot core type, size and μ_e value, and for a given type of winding conductor, a full winding of a particular conductor diameter will give a certain inductance and a corresponding Q curve. Round values of Q may be read off and plotted on inductance versus frequency coordinates for the particular inductance value. This may be repeated for the whole range of conductor sizes and corresponding inductances. The equal Q points may then be joined to give contours.

The 'hertz' (Hz) is the unit of frequency adopted internationally for the 'cycle per second' (c/s). 1MHz = 1Mc/s etc.

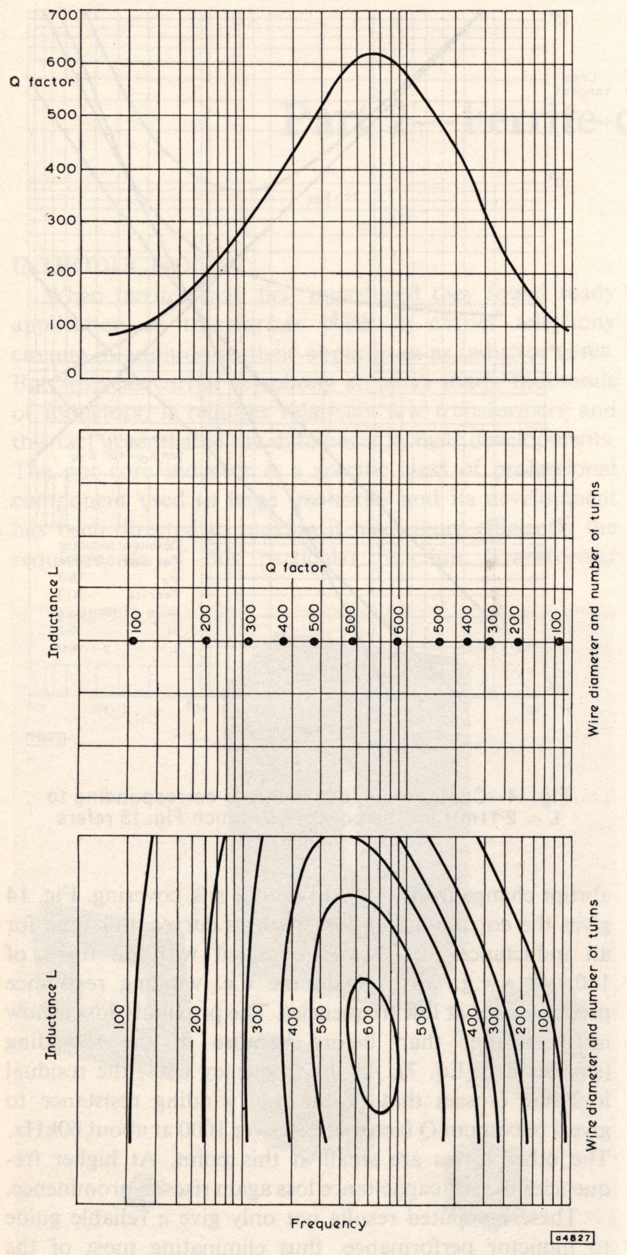

Fig. 10—Stages in the formation of an iso-Q chart

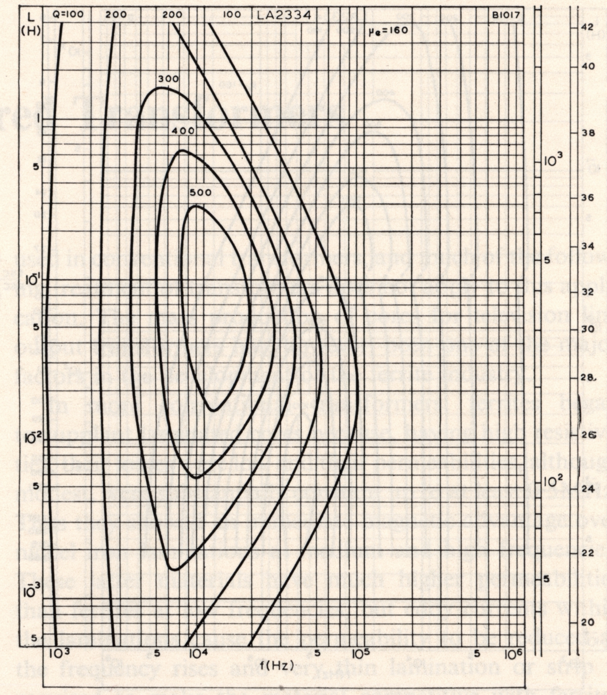

Fig. 11—Actual iso-Q chart for a particular 25mm pot core ($\mu_e = 160$) fully wound with solid wire. The ordinates indicate inductance, approximate number of turns, and s.w.g. number

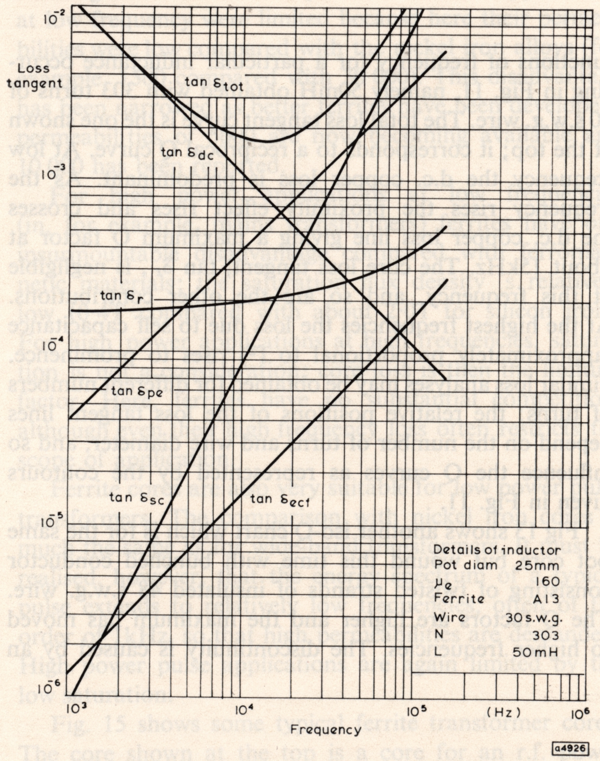

Fig. 12—Contributory loss tangents corresponding to L = 50mH for the pot core to which Fig. 11 refers

Fig. 11 shows an actual iso-Q chart for a 25mm pot core for which μ_e is 160, fully wound with enamel-covered solid wire. Fig. 12 shows the contributory loss tangents as

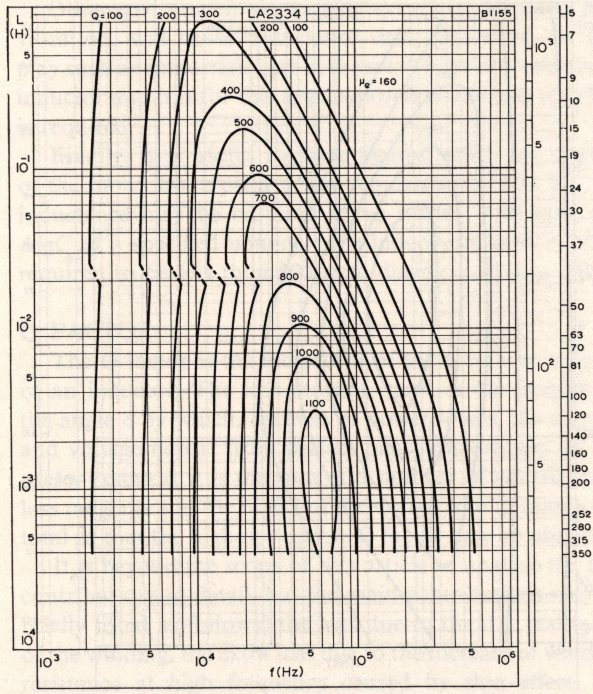

Fig. 13—Actual iso-Q for chart the pot core ($\mu_e = 160$) referred to in Fig. 11, but fully wound with 48 s.w.g. stranded wire. The ordinates indicate inductance, approximate number of turns, and number of strands

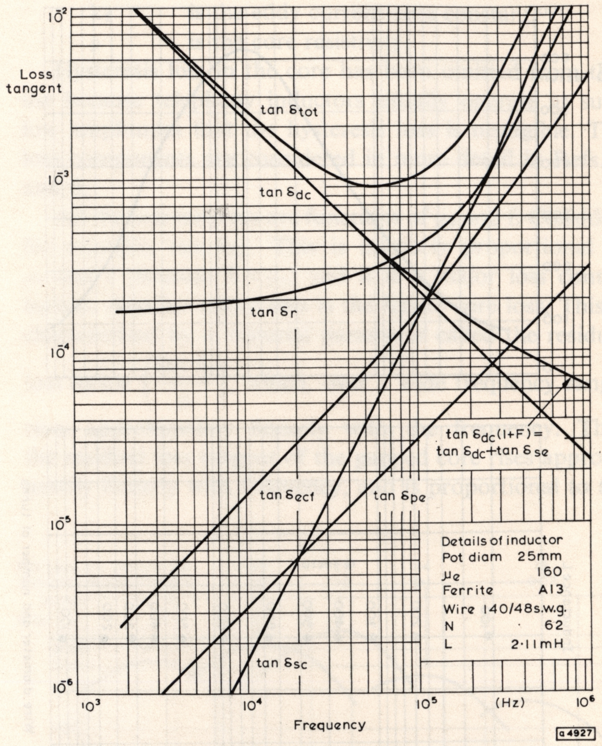

Fig. 14—Contributory loss tangents corresponding to L = 2·11mH for the pot core to which Fig. 13 refers

functions of frequency for a particular inductance occurring in Fig. 11, namely 50mH obtained with 303 turns of 30 s.w.g. wire. The total loss tangent curve is the one shown at the top; it corresponds to a reciprocal Q curve. At low frequency the d.c. copper loss is predominant. As the frequency rises the proximity effect rises and crosses the d.c. copper loss line giving a maximum Q factor at about 15kHz. The core loss tangent, tan δ_r, is negligible at this frequency, and so are the other contributions. At the highest frequencies the loss due to self capacitance (approximately proportional to f^2) rises to prominence. Similar loss analyses may be obtained for different numbers of turns; the relative positions of the loss tangent lines depend on the number of turns and wire diameter, and so influence the Q curves as represented by the contours given in Fig. 11.

Fig 13 shows another iso-Q chart which is for the same pot core but wound this time with bunched conductor consisting of twisted strands of insulated 48 s.w.g. wire. The Q factors are higher and the maximum has moved to higher frequencies. The discontinuity is caused by an abrupt change from single to double silk covering. Fig. 14 gives the corresponding loss analysis curves, this time for an inductance of 2·11mH obtained with 62 turns of 140×48 s.w.g. wire. Again the d.c. winding resistance predominates at low frequencies. The proximity loss is now much smaller than before because of the stranding (smaller d in Eq. 7). As the frequency rises, the residual loss line crosses that of the d.c. winding resistance to give a maximum Q factor of just over 1000 at about 60kHz. The other losses are small at this point. At higher frequencies the self capacitance loss again rises to prominence.

These computed results not only give a reliable guide to inductor performance, thus eliminating most of the labour of inductor design, but a comparative study gives a useful insight into the way in which the contributory losses affect the overall result.

This article surveys only very briefly present-day ferrite inductor practice, and highlights a few of the more important aspects. The references should be consulted if more detailed information is required.

Part 2—Ferrite-cored Transformers

INTRODUCTION

When ferrites were first introduced they found ready application as transformer cores in carrier telephony circuits in addition to their application as inductor cores. But whereas carrier telephony employs many thousands of inductors, it requires relatively few transformers and this fact accentuated the differences in their developments. The pot core inductor is a specific class of professional component used in large quantities and its development has been directed to making it meet more efficiently the requirements of this particular function. Transformer requirements in professional equipment are much more diverse and there has been no corresponding evolution of a class of core. It was in domestic television that the only mass application was found. The television line output transformer is a very specialised component. With its adjacent circuit, it is also a waveform generator and a high voltage generator. This results in a core shape and design procedure that are quite different from those used in conventional transformers, and much of the following treatment of transformers does not apply to this application. The mass production of cores for television line output transformers has, however, been one of the major factors in the development of the ferrite industry.

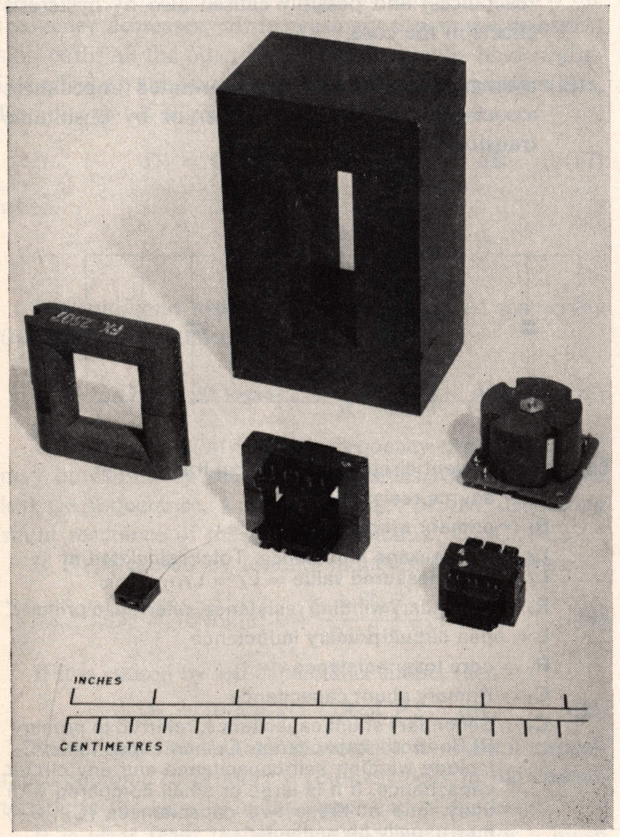

Fig. 15—Typical transformer cores

In more conventional transformers, ferrites began to supplant laminated cores because, having high resistivities, their losses were low and their permeabilities, although modest, were substantially constant up to at least 0·5MHz. Thus they showed an immediate magnetic advantage over nickel iron laminations at medium and high frequencies. These latter materials have much higher permeabilities than ferrites at low frequencies, but eddy currents within the laminations cause the permeability to be reduced as the frequency rises and very thin lamination or strip is required to make the material competitive with ferrites above some tens of kHz. Ferrites also have the practical advantage of avoiding the costly production process of stacking laminations. Low power wide-band applications at low frequency were limited because here their permeabilities were low compared with the nickel iron alloys (for example, 1500 compared with 30 000). This disadvantage has been narrowed as better ferrites have been developed; permeabilities of 5000 are now becoming available and 10 000 has been reported.

For high power applications at low frequencies (in, for example, mains transformers) ferrites have one insurmountable disadvantage compared with ferromagnetic materials; the saturation flux density is relatively low (0·4T compared with about 2·0T for silicon iron). For high power applications at high frequencies, saturation is not a consideration; core loss is then the limiting factor. Here, ferrites have no substantial competition, although even their high frequency loss often restricts the scope of application.

Ferrite cores are also very suitable for low power pulse transformers. The comparison with nickel iron cores is much the same as for wide-band transformers. It must be realised, however, that the energy spectrum of a typical pulse extends to relatively low frequencies, often of the order of 1kHz, so that high permeabilities are demanded. High power pulse applications are again limited by the low saturation.

Fig. 15 shows some typical ferrite transformer cores. The core shown at the top is a core for an r.f. power transformer; that on the left is a television line output transformer core. At the centre and the right are some medium frequency wide-band transformer cores, while at the bottom left there is a core specially designed for a particular r.f. wide-band application.

The 'tesla' (T) is the unit of magnetic flux density of one weber per square metre (Wb/m^2).

GENERAL CONSIDERATIONS

Fig. 16 shows a diagram representing a transformer between a source having resistance R_a and a load, R_b. If the reactances of the windings are so large that the magnetising current may be ignored, and if there are no imperfections such as winding resistance, leakage inductance or capacitance, then the input power equals the output power, the terminal voltages equal the winding e.m.f.'s and the transformation is perfect. That is,

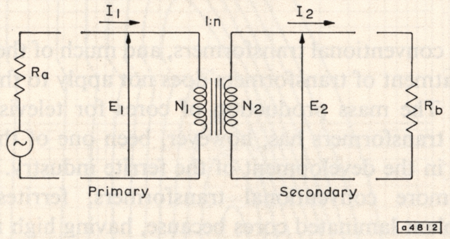

Fig. 16—Ideal transformer circuit

$$\frac{d\Phi}{dt} = \frac{E_1}{N_1} = \frac{E_2}{N_2}, \qquad \ldots(12)$$

where Φ is the flux in the core.

$$E_2 = nE_1 \qquad \ldots(13)$$

$$I_2 = \frac{I_1}{n} \qquad \ldots(14)$$

$$E_2I_2 = E_1I_1 \qquad \ldots(15)$$

and

$$\frac{E_1}{I_1} = \frac{R_b}{n^2} = R_b', \qquad \ldots(16)$$

where R_b' is the value of the load impedance as it appears at the input terminals.

In a practical transformer, however, the coupling is never complete, the winding reactances are finite and there are power losses caused by winding resistances and magnetic loss in the core. As a result, the above equations are not entirely valid. They can be made approximately true over a range of frequency, or $d\Phi/dt$ values, but this range is limited.

The practical transformer with all its imperfections may be represented by an equivalent circuit consisting of an ideal, or perfect, transformer and a number of lumped elements which represent the departures from the ideal transformer. Such a circuit is shown in Fig. 17. In practice, this circuit may usually be simplified when considering a particular aspect of the design.

The primary and secondary windings are invariably wound on a common magnetic core, the purpose of which is to provide adequate magnetic coupling. See Refs. 7 and 8 for further information on general transformer design.

WIDE-BAND TRANSFORMERS

Wide-band transformers are extensively used in communication networks to match load impedances to source impedances. They may also perform other functions, such as conversion from balance to unbalance, and d.c. isolation. The waveform is generally complex and constantly changing; the energy is distributed over a well-defined spectrum and the amplitude is usually low. An ideal transformer will transfer the energy without loss and without waveform distortion, and the load impedance will be perfectly transformed to the primary circuit. A practical transformer having the imperfections shown in Fig. 17 will introduce

(i) power loss, caused mainly by the winding resistance and possibly caused also by magnetic loss in the core,

(ii) waveform distortion, mainly caused by variation in the transfer impedance (which is frequency dependent because of the presence of unwanted reactances) and possibly caused also by hysteresis effects in the core,

(iii) mismatch caused by either unwanted impedances associated with the transformer or by unsuitable transformation ratio, or both.

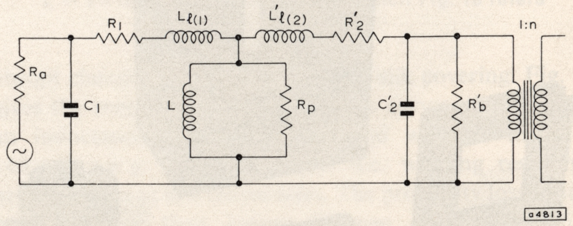

Fig. 17—Equivalent circuit of a practical transformer

R_a = source resistance

R_1 = primary winding resistance

$\left.\begin{matrix} L_{\ell(1)} \\ L_{\ell(2)}' \end{matrix}\right\}$ = leakage inductance. Total calculated or measured value = $L_\ell = L_{\ell(1)} + L_{\ell(2)}'$

R_2' = secondary winding resistance, referred to primary′

L = open circuit primary inductance

R_p = core loss resistance

C_1 = Primary shunt capacitance

C_2'= Secondary shunt capacitance, referred to primary (N.B.—Both capacitance C_1 and capacitance C_2' include winding self-capacitance and any circuit capacitance. If n is large or small compared with unity, one of these two capacitances (C_1, C_2') may usually be neglected

R_b' Load resistance referred to primary

Designing a transformer to have a specified performance in all these respects can be a long and difficult job. However, it is often sufficient to meet relatively few requirements. The most usual specification relates to the transmission frequency characteristic; it lays down the minimum transmission band and usually sets a limit to the mid-band loss.

Fig. 18 shows a transformer frequency characteristic expressed in a conventional way for transformers. The ordinate is the insertion loss of the transformer relative to that of an ideal transformer; it is the ratio of the voltage across the load relative to the voltage that would appear if the transformer were perfect and of the correct matching ratio. The loss is expressed in decibels. The droop at the lower frequency end of the band is caused by the shunt reactance of the transformer (that is, L in Fig. 17). As the frequency decreases, ωL increasingly shunts the transmission path; all the other imperfections usually have negligible effect on the low frequency droop. The insertion loss, D_1, due to ωL is given by

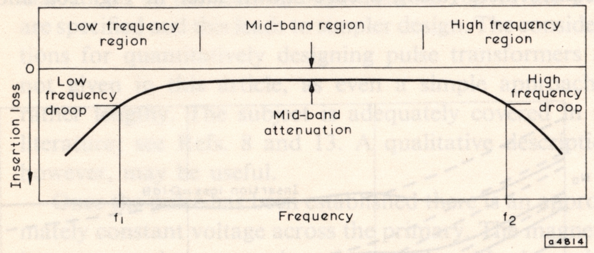

Fig. 18—General shape of transformer insertion loss curve

$$D_1 = 10\log_{10}\left(1 + \frac{R^2}{\omega^2L^2}\right) \quad \text{dB} \qquad \ldots(17)$$

where

$$R = \frac{R_aR_b'}{R_a + R_b'}.$$

The mid-band loss, D_m, is usually caused mainly by the winding resistance, and is given by

$$D_m = 20\log_{10}\left(1 + \frac{R_1 + R_2'}{R_a + R_b'}\right) \quad \text{dB}. \qquad \ldots(18)$$

The droop, D_2, at the high frequency end of the band may be caused by the increasing series reactance of the leakage inductance, $L = L_{\ell(1)} + L_{\ell(2)}'$, or the decreasing shunt reactance of the shunt capacitance, $C = C_1 + C_2'$.

If D_2 is caused by leakage inductance alone, then

$$D_2 = 10\log_{10}\left(1 + \frac{\omega^2L_\ell^2}{(R_a + R_b')^2}\right) \text{dB}. \qquad \ldots(19)$$

If it is caused by self capacitance alone, then

$$D_2 = 10\log_{10}\{1 + (R\omega C)^2\} \quad \text{dB}. \qquad \ldots(20)$$

Sometimes the leakage inductance and shunt capacitance combine to produce a resonant peak in the characteristic in the vicinity of the upper end of the band.

It is clear from the above equations that for a given transformer the insertion loss depends on the source and load impedances. Clearly if the load impedance is infinite the effect of the series impedance, R_1, R_2' and L_ℓ, is zero, while if the source impedance is zero the shunt impedances have no effect.

For a given core and a given winding arrangement, the ratio L/L_ℓ is independent of the number of turns. It follows that the bandwidth ratio f_2/f_1 is correspondingly constant if the self-capacitance can be disregarded. The more turns or the lower the circuit impedance, the lower in frequency is the pass-band placed. For a reasonably good transformer L/L_ℓ would be about 1000 and the corresponding f_2/f_1 ratio referred to the 1 dB points would be 1000 for a matched circuit.

The bandwidth may, in general, be increased by using a larger core, or by using a higher permeability core material; these changes increase L. Alternatively, reference to leakage inductance calculations (Ref. 9) shows that increasing the winding breadth/height ratio, or splitting the primary and secondary into alternately sandwiched sections, will reduce L_ℓ and will therefore also increase f_2/f_1. Although within the above conditions f_2/f_1 is independent of the position of the passband, as the position of the passband is moved to higher frequencies the presence of shunt capacitance will limit the maximum value of f_2. It can be shown that for a given core shape $L_\ell.C_s$ is roughly constant (C_s being the self-capacitance of the windings). Any change in winding geometry designed to reduce L_ℓ will increase C_s. The leakage inductance increases as N^2, and the self-capacitance tends to increase with N, so it it best to use the least possible number of turns if the highest value of f_2 is required. The choice of core material may be regarded as a means of reducing the required number of turns. One uses the core with the highest available effective permeability and calculates, from the inductance factor, the number of turns to give a shunt inductance that will just ensure that the specification at f_1 is satisfied. If the specification at f_2 cannot be met with a reasonable winding arrangement then a more suitable core must be used.

The inductance factor, that is, the factor connecting the number of turns with the inductance obtained on a given core, is usually constant for manganese zinc ferrites up to frequencies of at least 500kHz. Material permeabilities of 2000 are readily available and cores with material permeabilities of 5000 are becoming available.

From the earlier discussion it may appear that any size of core may be used to make a transformer having a reasonable pass-band, however low the pass-band frequency is. It seems necessary only to wind on enough turns to get a sufficient inductance. However, the more turns that are used the thinner the conductor must be; it is easily shown that, for a given core size, the winding resistance is proportional to N^2. If the winding resistance is appreciable in relation to the circuit impedance then an excessive mid-band loss will occur. If the mid-band loss must be made smaller, other things being equal, then a larger core or a higher effective permeability is necessary. The shunt resistance R_p in Fig. 17 represents the core loss and this may be taken into account if desired. Although normally negligible it may contribute an additional mid-band loss.

The following paragraphs summarise the simple design procedure for medium frequency wide-band transformers

(a) Calculate minimum primary inductance from Eq.17. Assume a core (see Ref. 10 for typical ferrite cores) and calculate the number of primary turns. From the required turns ratio calculate the number of secondary turns.

(b) For a simple transformer, allow half the winding space for each winding, calculate suitable conductor diameters and, from the mean turn length, estimate the winding resistances. Using Eq.18, check that the mid-band loss is satisfactory. If not, repeat design using a larger core.

(c) Calculate leakage inductance (Ref. 9) and estimate the total winding capacitance from Ref. 11 (normally only the self-capacitance of the high impedance winding need be considered). Using Eqs.19 and 20, check whether L_ℓ and C will give a satisfactory insertion loss at f_2. If the leakage inductance is too high, divide the windings into alternate horizontal sections as discussed in Ref. 9. If the self-capacitance is too high then the windings may be divided into vertical sections as shown in Ref. 11. If the characteristic at f_2 cannot be achieved by either of these courses then it is probable that the bandwidth requirement is rather severe and, if a better core cannot be found, then perhaps filter techniques must be used (See Ref. 12).

Fig. 19 shows typical insertion loss curves for transformers using high permeability ferrite pot cores; in both cases $f_2/f_1 > 1000$. These curves are plotted in the manner conventional for filters, that is, upside down with respect to Fig. 18.

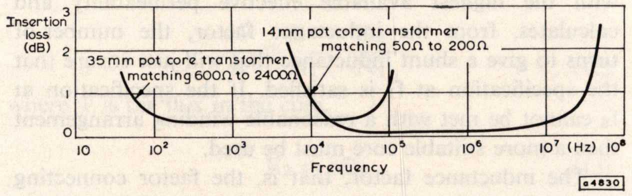

Fig. 19—Insertion loss of typical wide-band transformers using pot cores

The approach described so far is for medium frequency transformers, that is, those in which the lower pass-band frequency is below the value at which the ferrite permeability starts to fall. For higher frequency wide-band transformers, the droop at f_1 depends on both L and R_p in Fig. 17 and both are functions of frequency. Maurice and Minns (Ref. 12) suggested a design procedure. A hypothetical transformer having unity ratio is assumed to be connected between 1Ω resistances. The core of the transformer is assumed to have $\Sigma(\ell/A)$ (that is, reluctance normalised with respect to permeability) equal to unity. The number of turns, N_a, required to obtain a given insertion loss may be calculated from the magnetic properties of the core and plotted as a function of frequency. To obtain the same insertion loss at a given frequency with an actual core, having $\Sigma(\ell/A) = C_1$, connected between a source and load each having resistance R, the actual number of turns N is given by

$$N = N_a\sqrt{(RC_1)}\,. \qquad \ldots(21)$$

If the ratio is not unity, R is twice the value of the parallel combination of source and load resistances referred to the winding being calculated. Fig. 20 shows such curves for two ferrites suitable for h.f. wide-band transformers. One is high permeability manganese zinc ferrite and the other is a high permeability nickel zinc ferrite. For a given insertion loss, the material having the lower value of N_a at the required f_1 frequency is the more suitable.

Fig. 21 shows typical characteristics of h.f. wide-band transformers (using a core shown later in Fig. 26a and described in a later section). Again a bandwidth of over three decades is achieved, this time with a highest frequency in the region of 200MHz.

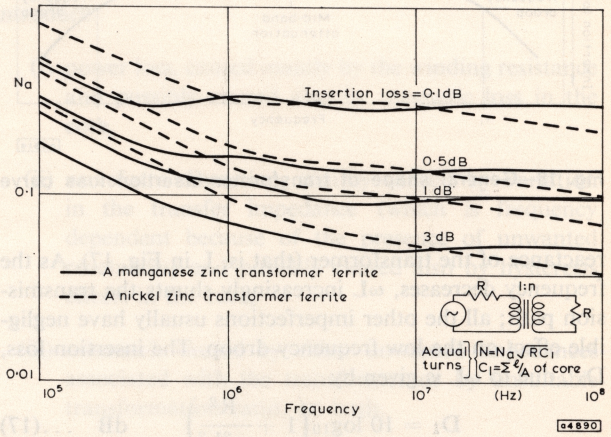

Fig. 20—Normalised number of turns (N_a) plotted against frequency

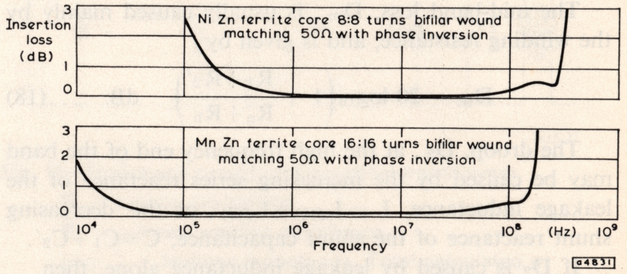

Fig. 21—Insertion loss characteristics of typical wide-band transformers using the core shown in Fig. 26a on page 42

LOW-POWER PULSE TRANSFORMERS

Pulse transformers, like wide-band transformers, are required to transmit energy which is distributed over a wide frequency spectrum, but instead of the performance being specified in terms of this spectrum it is specified in terms of its effect on a given wave or pulse of current or voltage expressed as a function of time. The time function usually approximates to a rectangular pulse and the purpose of the transformer is to transfer the energy from the primary circuit, often the pulse generating circuit, to the secondary or load circuit without excessive distortion. Fig. 22 shows a typical perfect and a distorted version of the pulse, and illustrates some definitions.

Just as, in the case of the wide-band transformer, it was possible to treat the low, medium and high frequency parts of the specification separately, so one may treat the leading edge, the top of the pulse and the trailing edge separately. If all three parts are fully specified, the design procedure is difficult. In many cases, however, only the distortions of the leading edge and the top of the pulse are specified and this leads to simpler design. The considerations for quantitatively designing pulse transformers are not given in this article, as even a simple approach is rather lengthy. The subject is adequately covered in the literature; see Refs. 8 and 13. A qualitative description, however, may be useful.

Once the pulse has been established there is an approximately constant voltage across the primary. The magnetising current rises approximately linearly with time, since $E = L\,di/dt$. This current has to be supplied by the source but it does not reach the load, so the output amplitude progressively falls. This droop is equivalent to a low frequency characteristic: the higher the shunt inductance is, the less the droop. One object in pulse transformer design is to make the primary inductance high enough, but not too high as this would jeopardise the higher frequency components of the waveform. If the permissible droop is D% in time t_d, and R equals $R_aR_b'/(R_a+R_b')$, then the required inductance L is given by:

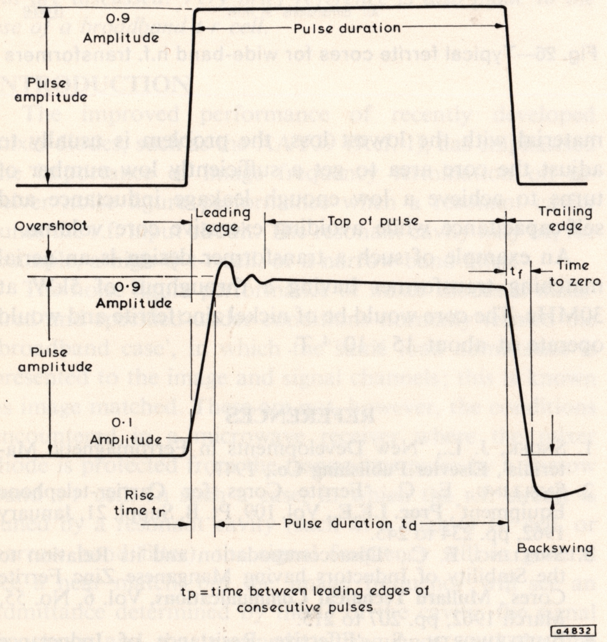

Fig. 22—Pulse shapes before and after passing through a transformer

$$L = \frac{-t_dR}{\log_e(1-D/100)}\,. \qquad \ldots(22)$$

This inductance must be achieved with the minimum of leakage inductance if a steep leading edge is required. The shape of the leading edge is determined by the self capacitance, which is being charged through the leakage inductance. If the transformer is matched, the rise will be aperiodic and it might have up to about 4·5% over-shoot. The smaller the leakage inductance is, the faster the rise-time. Thus, as for the wide-band transformer, a high value of L/L_ℓ is required. Much of the discussion of L/L_ℓ in the section on wide-band transformers applies here also.

One practical design procedure is to wind a trial transformer having the required shunt inductance and the lowest possible leakage inductance, that is, with each winding a single layer. It is then put into the circuit and the response is observed. If the over-shoot is oscillatory the transformer is not matching the source and load. If this cannot be remedied, then shunt capacitance may be added until the over-shoot response is acceptable. If the rise time is then too slow a larger core or one with higher effective permeability must be used.

CORES FOR LOW-POWER TRANSFORMERS

In the foregoing sections the need for a high ratio of shunt inductance to leakage inductance has been stressed. Core shapes providing wide and shallow winding area will give low leakage inductance, but there is not much room for manoeuvre in this respect. A core should, for its size, give a high inductance for a given number of turns; thus, the core should, as previously stated, reduce the necessary number of turns to a minimum. Since the leakage inductance is proportional to N^2 this will increase L/L_ℓ.

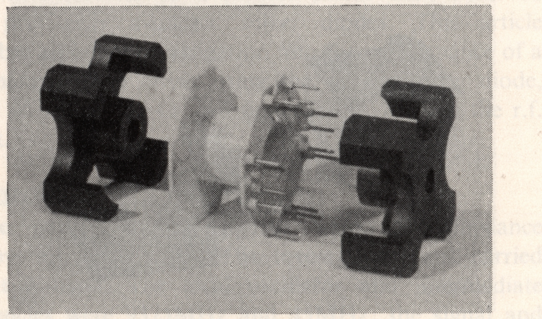

Fig. 23—Example of an X core

Since both the inductance and the winding resistance are proportional to N^2, the ratio R/L is a constant for a core. The lower this value, the lower will be the mid-band loss for a given frequency band.

Ferrite transformer cores were first made in a variety of E core shapes corresponding to the standard laminations. The versatility of solid pressed cores was then exploited, first with E cores having round centre legs and later with even more functional shapes. Fig. 23 shows an 'X core', designed to utilise fully the available volume and to provide space for a coil former having fixed pins compatible with printed wiring technology.

Cores such as those mentioned in the preceding paragraph might have material permeabilities of about 2000. Because of the unavoidable residual gap at the mating surfaces of the half cores, the corresponding effective permeability might be only 1500. As the material permeability increases, so the loss of effective permeability due to the gap becomes more serious. Fig. 24 illustrates this point. A material permeability of 5000 may be obtained but it is difficult to exploit it. Fig. 25 shows one solution. It is, in effect, a shallow U and an I core in which the serifs of the I have been lengthened to form an H. The U core has been correspondingly broadened so that the mating surfaces are greatly increased in area. In addition, the mating surfaces are lapped to optical flatness. Thus the reluctance, ℓ/A, of the gaps is greatly reduced and effective permeabilities of over 4500 are attainable with material permeabilities of about 5000. This core is very compact and is very suitable for wide-band and pulse transformers requiring high inductances.

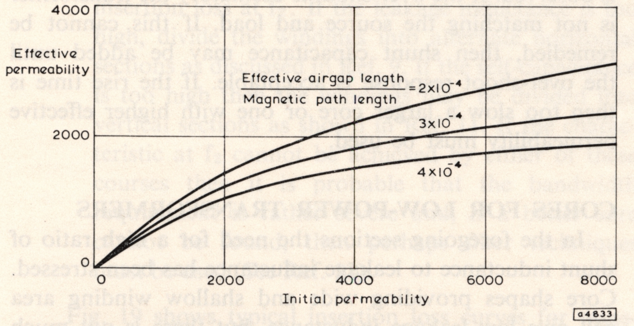

Fig. 24—Effective permeability plotted as a function of initial permeability and unavoidable air gap

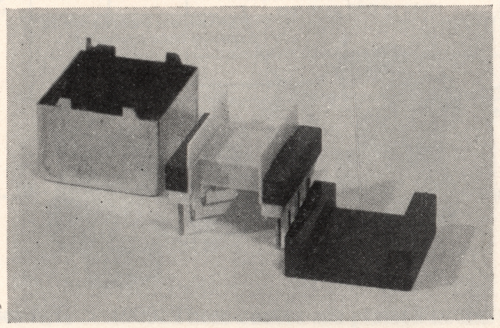

Fig. 25—Example of an H core

For h.f. wide-band transformers, or pulse transformers for very short pulses, an alternative approach is to avoid the gap entirely and design the core as a single or double toroid, optimised to give the highest inductance per unit length of winding wire. Such cores, which have the form of one- or two-hole beads, are illustrated in Fig. 26. For h.f. transformers, they require only a few turns and these are easily threaded by hand. Some typical wide-band characteristics obtainable with the one-hole bead are shown in Fig. 21.

H.F. POWER TRANSFORMERS

Transformers in this category include ultrasonic output transformers, and aerial matching transformers for radio transmitters. Ferrite cores are invariably used. In order to avoid excessive size, the cores are run at the highest flux density permitted by loss and heating considerations; at high frequencies, losses limit the flux density long before saturation is reached. If $\hat{B}$ is the flux density corresponding to an acceptable loss density, then the number of turns is determined by the e.m.f. equation:

$$E = \frac{\omega \hat{B} A N}{\sqrt{2}} \text{volts} \qquad \ldots(23)$$

where $\hat{B}$ is in T

A is the core area in m².

This number of turns is usually more than the number required for adequate shunt inductance. Given the material with the lowest loss, the problem is usually to adjust the core area to get a sufficiently low number of turns to achieve a low enough leakage inductance and self-capacitance while avoiding excessive core volume.

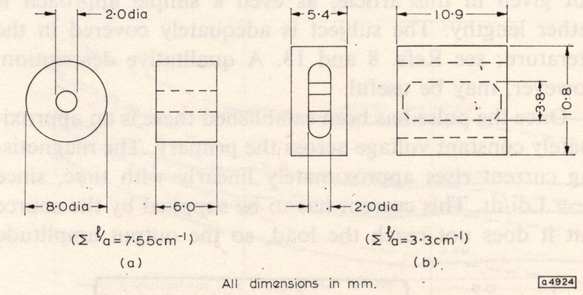

(a) (b)

Fig. 26—Typical ferrite cores for wide-band h.f. transformers

An example of such a transformer design is an aerial matching transformer having a throughput of 5kW at 30MHz. The core would be of nickel zinc ferrite and would operate at about 15×10^{-4} T.

REFERENCES

1. Snoek, J. L., 'New Developments in Ferromagnetic Materials', **Elsevier Publishing Co.**, 1947.
2. Snelling, E. C., 'Ferrite Cores for Carrier-telephone Equipment', **Proc. I.E.E.**, Vol. 109, Pt. B, Suppl. 21, January 1962, pp. 234 to 245.
3. Snelling, E. C., 'Disaccommodation and its Relation to the Stability of Inductors having Manganese Zinc Ferrite Cores', **Mullard Technical Communications**, Vol. 6, No. 55, March 1962, pp. 207 to 215.
4. Butterworth, S., 'Effective Resistance of Inductance Coils at Radio Frequency', **Experimental Wireless and the Wireless Engineer**, Vol. 3, No. 31, April 1926, pp. 203 to 210, *ibid.* No. 32, May 1926, pp. 309 to 316.
5. Welsby, V. G., 'The Theory and Design of Inductance Coils', **MacDonald and Co.**, 2nd. ed., 1960.
6. Mullard Technical Handbook, Vol. 6, Introductory Notes etc., Vinkor Adjustable Pot Core.
7. MacFadyen, K. A., 'Small Inductors and Transformers', **Chapman and Hall**, 1953.
8. Lee, R., 'Electronic Transformers and Circuits', **Chapman and Hall**, 1947.
9. Crowhurst, N. H., 'Leakage Inductance', **Electronic Engineering**, Vol. 21, No. 254, April 1949, pp. 129 to 134.
10. Mullard Technical Handbook, Vol. 6, Introductory Notes etc., Transformer Cores.
11. Duerdoth, W. T., 'Equivalent Capacitances of Transformer Windings', **Wireless Engineer**, Vol. 23, No. 273, June 1946, pp. 161 to 167.
12. Maurice, D., and Minns, R. H., 'Very-wide Band Radio Frequency Transformers', **Wireless Engineer**, Vol. 24, No. 285, June 1947, pp. 168 to 177, *ibid.*, No. 286, July 1947, pp. 209 to 216.
13. Wilds, C. F., 'Determination of Core Size in Pulse Transformer Design', **Electronic Engineering**, Vol. 33, No. 403, September 1961, pp. 566 to 573.

Performance of AAY39 Mixer Diode with Narrow Band T-R Cell

T. H. Oxley and R. W. Yell

Wembley Laboratories, Associated Semiconductor Manufacturers Ltd.

The performance of the Mullard AAY39 diode as a mixer in the X-band is examined in conjunction with a narrow band t-r cell. Experimental results are given for a single-ended mixer, a balanced mixer, and a mistuned r.f. input circuit. Dynamic performance, 'temporary deterioration', and burn-out are discussed. Very brief reference is also made to the use of a broadband t-r cell.

INTRODUCTION

The improved performance of recently developed mixer diodes, such as the AAY39 (Ref. 1), has emphasised the importance of image frequency termination on receiver noise figure performance when a resonant cavity tunes the r.f. input circuit. The resonant cavity may be, for example, a high-Q t-r cell, or a narrow band filter.

The noise figure performance of mixer diodes is measured and specified under conditions normally termed the 'broadband case', in which the same load admittance is presented to the image and signal channels; this is known as image matched. These are not, however, the conditions encountered in a microwave receiver where the mixer diode is protected from the transmitter pulse by a narrow band t-r cell. In such a case, in which the r.f. circuit is tuned by a resonant cavity (such as a high-Q t-r cell, or narrow band filter), the signal frequency will in general see a near match, but the image frequency will see an admittance determined by the Q of the cavity, the signal frequency and the intermediate frequency, and the line length from the cavity to the reference terminals of the mixer. If this line length is varied, the image load admittance can become almost a short circuit or an open circuit; this will affect the mixer conversion efficiency and the intermediate frequency impedance. The variation in i.f. impedance may, in turn, affect the performance of the succeeding i.f. amplifier. The extent of these effects is dependent on the conversion loss of the mixer diode and becomes more severe as this loss is reduced. However, theoretically, it should be possible to use the above effects to advantage in improving the overall noise figure performance of the receiver (Ref. 2) in the following way. Conversion of signal power to the intermediate frequency entails the production of power at the image frequency. In the image matched conditions this power is dissipated in the image termination; however, if the power at the image frequency is reflected back into the mixer diode in the same voltage phase (that is, image open circuit) this power may also be converted to the intermediate frequency. Accompanying this improvement in conversion efficiency there is an increase in the intermediate frequency impedance of the diode and, consequently, an increase in the diode noise temperature ratio.

The conversion loss of the AAY39 in the image matched condition is about 4dB. Thus it was recognised that the termination of this diode when used in conjunction with a narrow band t-r cell could affect the performance of a microwave receiver to a greater extent than observed with previously available mixer diodes. This article describes an initial investigation into the performance of a superheterodyne receiver using the AAY39 mixer diode, and a narrow band t.r. cell type QF45X to tune the r.f. circuit.

EXPERIMENTAL RESULTS

The parameters investigated were i.f. impedance and overall noise figure. The investigation was carried out at X-band. The local oscillator and intermediate frequencies were 9375MHz and 45MHz: the signal and image frequencies 9420MHz and 9330MHz respectively.

The resonant cavity used to tune the r.f. circuit was a narrow band t-r cell type QF45X, with the following characteristics.

Insertion loss	0·52dB
Loaded Q	130
Spike leakage	0·04 erg/spike

The phase of the image reflection from the cavity was varied by a phase shifter.

The signal source was a noise tube type CV1881, with a calibrated noise power of 15·5dB above thermal level. In the broadband case this noise power is available at both signal and image channels and hence 18·5dB is the available noise power for the receiver noise figure calculations. When the t-r cell tunes the r.f. input, only 0·5dB of the noise power is available at the image channel and thus 16·0dB is the total available noise power. This value was substantiated by receiver noise figure measurements under broadband and image matched conditions. In the latter case, the t-r cell tuned the r.f. input, but an isolator was included in the circuit to absorb the image reflection. Excellent agreement was observed in noise figure performance, referred to the mixer terminals, for both cases.

Single-ended Mixer

Fig. 1 is a schematic diagram of the measurement apparatus. The 45MHz i.f. amplifier was of conventional thermionic valve design with a noise figure of about 2dB at the optimum source impedance. The diode holder was a waveguide type mount designed for test purposes. With local oscillator drive, the diodes have a v.s.w.r. better than 1·43 : 1 with respect to this mount; no further matching was carried out.

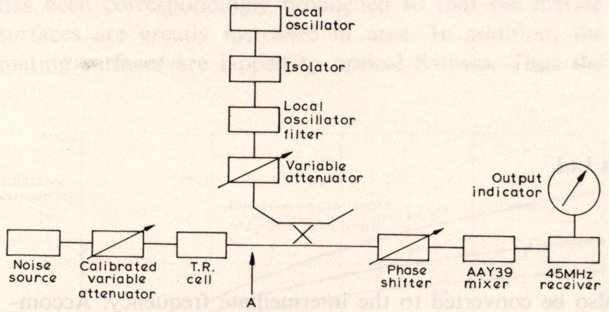

Fig. 1—Measurement apparatus for AAY39 single-ended mixer

For broadband measurements the t-r cell was removed. For image matched measurements an isolator was inserted at point A.

The measurements made were of i.f. impedance and noise figure as a function of phase of the image reflection. Fig. 2 summarises the results, and identifies the image open circuit and short circuit conditions; these are maximum i.f. impedance with minimum noise figure, and minimum i.f. impedance with maximum noise figure respectively.

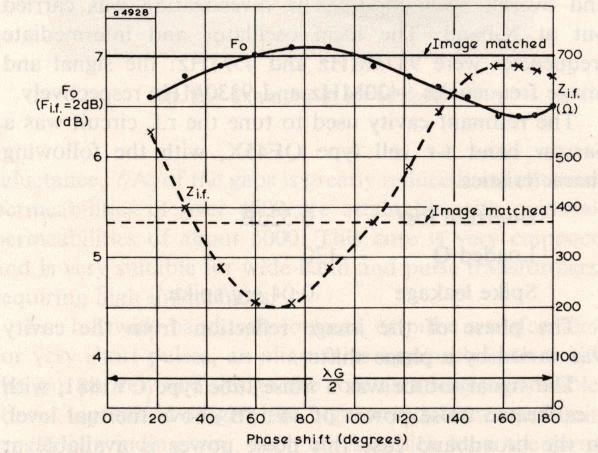

Fig. 2—Overall noise figure performance and i.f. impedance plotted as functions of phase of image reflection, for AAY39 single-ended mixer and t-r cell QF45X. The noise figure performance includes 0·5dB insertion loss of the t-r cell. Diode rectified current = 1·0mA

The results illustrate the effect on receiver performance of varying the line length from the cavity to the mixer terminals, and indicate the necessity of optimising this distance and the i.f. amplifier input impedance. Further, by optimum 'line stretching', an improved noise figure performance of at least 0·5dB compared with the image matched conditions is suggested, provided the input impedance to the i.f. amplifier is adjusted accordingly. This is sufficient to compensate for the insertion loss of the t-r cell, thus giving a receiver overall noise figure performance of about 6·5dB (noise figure of i.f. amplifier, $F_{i.f.}$ = 2dB) including the insertion loss of the cell.

The consistency in the performance of an image open circuit receiver was assessed by measurement of overall noise figure for a number of AAY39 diodes. In each case at least 0·5dB improvement was obtained compared with their image matched performance without any further adjustment of the receiver.

Balanced Mixer

Fig. 3 is a schematic diagram of the measurement apparatus. The balanced mixer was of R.R.E. design. The 45MHz i.f. amplifier incorporated a specially made transistor pre-amplifier. The noise figure was 1·4dB for a source resistance range of 175Ω to at least 600Ω.

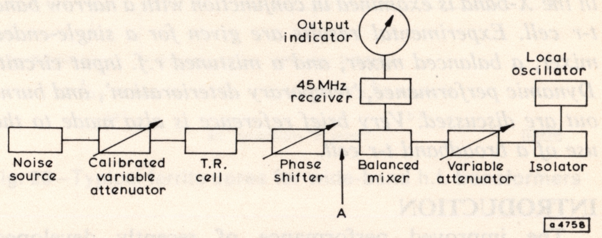

Fig. 3—Measurement apparatus for AAY39 balanced mixer

For broadband measurements the t-r cell was removed. For image matched measurements an isolator was inserted at point A.

Measurements were made of overall noise figure performance as a function of phase of the image reflection. Fig. 4 summarises the results. These confirm the evidence of the previous section and indicate the need of optimum 'line stretching' to provide low noise figure performance.

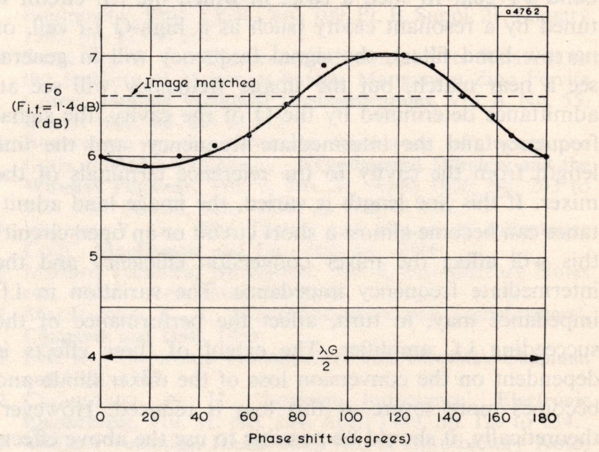

Fig. 4—Overall noise figure performance plotted as a function of phase of image reflection, for AAY39 balanced mixer (R.R.E. design and construction), 45MHz transistor pre-amplifier, and t-r cell QF45X. The noise figure performance includes 0·5dB insertion loss for the t-r cell. Diode rectified current = 1·0mA

A receiver noise figure performance of about 6·0dB ($F_{i.f.}$ = 1·5dB), including the insertion loss of the t-r cell, is illustrated. The degradation in performance at the image short circuit conditions is caused by the deterioration in the i.f. amplifier noise figure performance for the balanced i.f. impedance of about 100Ω.

Mistuning the R.F. Input Circuit

Fig. 5 shows the degradation in performance of the reciever caused by mistuning the r.f. input. A comparison is made of image matched and image open circuit conditions. Use of image open circuit does not further degrade the receiver performance compared with the image matched conditions in this respect.

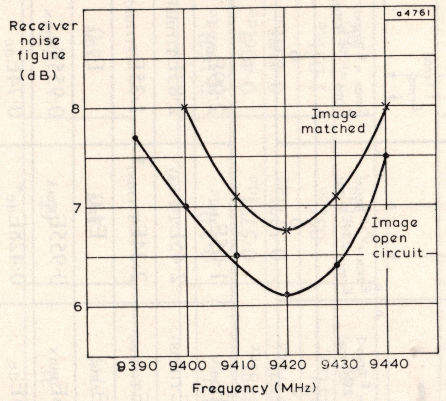

Fig. 5—Receiver noise figure performance plotted as a function of tuning of r.f. input

Dynamic Noise Figure Performance

It is known that with use of some mixer diodes there is a temporary increase in their noise figure performance after incident pulse powers. This is below the level at which permanent damage is caused and has become known as 'temporary deterioration'. A brief investigation was therefore carried out in this respect for the AAY39 in conjunction with the t-r cell type QF45X.

Fig. 6 is a schematic diagram of the measurement apparatus. The transmitter supplied peak powers of 3·5kW at a repetition rate of 2000p/s, pulse duration 0·5μs and frequency 9420MHz.

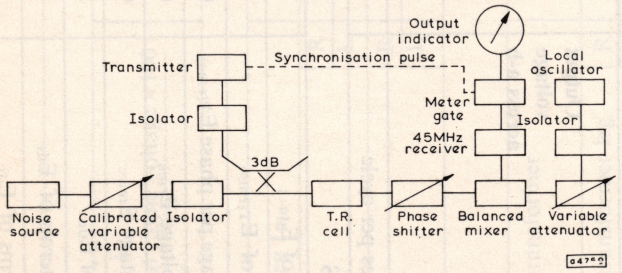

Fig. 6—Measurement apparatus for measuring 'temporary deterioration' of AAY39 diode under dynamic condition in a balanced mixer

Measurements were carried out using the balanced and single-ended mixers, under image matched, image open circuit and image short circuit conditions. No temporary deterioration was observed under any of these conditions.

Burnout

Burnout tests or permanent deterioration in diode performance caused by incident pulse powers have been carried out by Ferranti Ltd. The results have indicated a satisfactory life performance up to 500 hours for the AAY39, single-ended, behind the t-r cell QF45X.

PERFORMANCE WITH BROADBAND T-R CELL

Tests including burnout and temporary deterioration of the AAY39 in conjunction with the broadband t-r cell CV2311 and narrow band filters are in progress. Full results are not yet available. However, as the preliminary results may be of interest, these have been included here.

Briefly, the investigation has at present emphasised the importance of the bandwidth of the r.f. circuit following the t-r cell on the protection afforded by the t-r cell. This is summarised tentatively in Table 1.

TABLE 1

Performance of AAY39 Mixer with Broadband T.R. Cell

Bandwidth	T-R cell leakage for 10% diode failure
30%	0·075 erg/spike
10%	0·15 erg/spike
3%	>0·2 erg/spike

The burnout of the AAY39 when used in conjunction with its broadband waveguide test holder (30% r.f. bandwidth) appears to be inferior to the burnout when used in conjunction with the bar and post type mount (10% r.f. bandwidth). Again, the protection may be further improved by restricting the r.f. bandwidth by use of a narrow band filter; no diode failures have been recorded for the AAY39 in conjunction with its broadband waveguide mount and narrow band filter (3% r.f. bandwidth and 0·8dB insertion loss), behind a cell with a leakage of about 0·24 erg/pulse.

It is expected that the full result of these tests with a broadband t-r cell will be available at a later date.

ACKNOWLEDGEMENT

Acknowledgement is made to Mr. I. Bagnall of R.R.E. for the balanced mixer assembly and to Mr. J. G. Sommerville of Ferranti Ltd. for the t.r. cell.

REFERENCES

1. Oxley, T., 'Recent Advances in Germanium Microwave Mixer Diodes', **Mullard Technical Communications**, Vol.8, No. 78, November 1965, pp. 239 to 248.
2. Torrey, H. C. and Whitmer, C. A. 'Crystal Rectifiers'. **M.I.T. Radiation Laboratory Series** No. 15, McGraw-Hill, 1948.

IDEALISED RECTIFIER CIRCUIT PERFORMANCES *Revised version of table originally published in Vol. 7, No. 68, January 1964*	**Single-phase**			**Three-phase**			
	Half-wave	**Centre-tap full-wave**	**Full-wave bridge**	**Half-wave**	**Full-wave bridge**	**Centre-tap**	**Double-star with interphase transformer**
Type of rectifier circuit	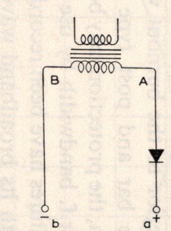	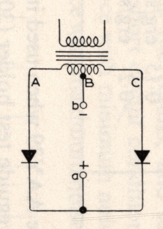	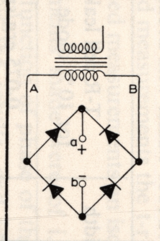	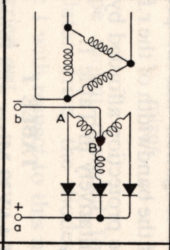	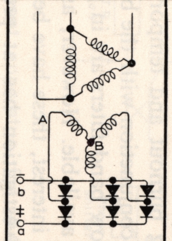	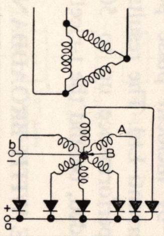	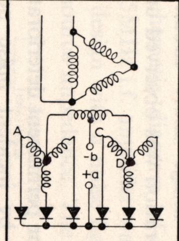
Secondary input voltage per phase	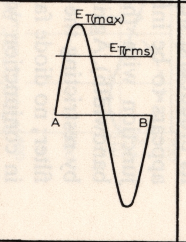	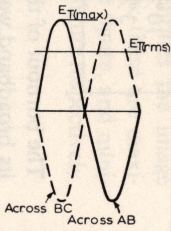	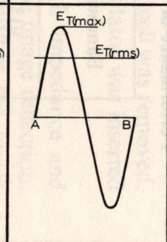	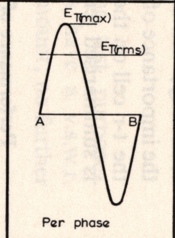	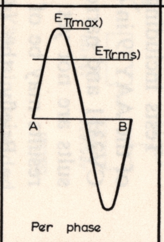	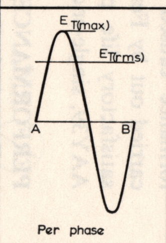	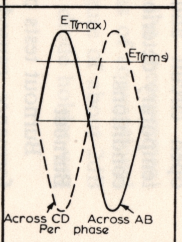
Output voltage across a-b	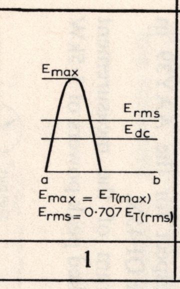	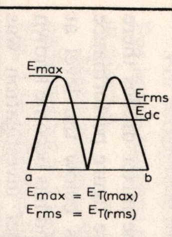	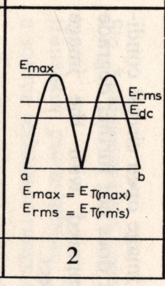	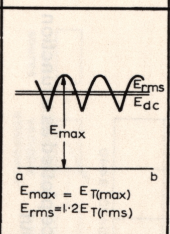	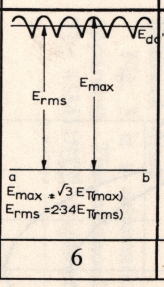	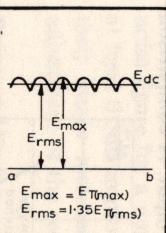	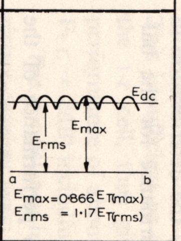
Number of output voltage pulses per cycle	1	2	2	3	6	6	6
VOLTAGE RELATIONSHIPS							
Crest working voltage in terms of E_{dc}	3·14E_{dc}	3·14E_{dc}	1·57E_{dc}	2·09E_{dc}	1·05E_{dc}	2·09E_{dc}	2·42E_{dc}
Crest working voltage in terms of $E_{T(rms)}$	1·41$E_{T(rms)}$	2·82$E_{T(rms)}$	1·41$E_{T(rms)}$	2·45$E_{T(rms)}$	2·45$E_{T(rms)}$	2·83$E_{T(rms)}$	2·83$E_{T(rms)}$
E_{dc} in terms of r.m.s. input voltage per phase $E_{T(rms)}$	0·45$E_{T(rms)}$	0·90$E_{T(rms)}$	0·90$E_{T(rms)}$	1·17$E_{T(rms)}$	2·34$E_{T(rms)}$*	1·35$E_{T(rms)}$	1·17$E_{T(rms)}$
E_{dc} in terms of r.m.s. output voltage E_{rms}	0·636E_{rms}	0·90E_{rms}	0·90E_{rms}	0·98E_{rms}	E_{rms}	E_{rms}	E_{rms}
E_{dc} in terms of peak output voltage E_{max}	0·318E_{max}	0·636E_{max}	0·636E_{max}	0·826E_{max}	0·955E_{max}	0·955E_{max}	0·955E_{max}
Input voltage $E_{T(rms)}$ in terms of E_{dc}	2·22E_{dc}	1·11E_{dc}	1·11E_{dc}	0·855E_{dc}	0·428E_{dc}*	0·74E_{dc}	0·855E_{dc}
R.M.S. output voltage E_{rms} in terms of E_{dc}	1·57E_{dc}	1·11E_{dc}	1·11E_{dc}	1·02E_{dc}	1·00E_{dc}	1·00E_{dc}	1·00E_{dc}
Peak output voltage E_{max} in terms of E_{dc}	3·14E_{dc}	1·57E_{dc}	1·57E_{dc}	1·21E_{dc}	1·05E_{dc}	1·05E_{dc}	1·05E_{dc}

RIPPLE								
Fundamental ripple frequency f_r		f	2f	2f	3f	6f	6f	6f
$\%\ \text{ripple} = \dfrac{\text{r.m.s. fundamental ripple voltage} \times 100}{E_{dc}}$		111	47·2	47·2	17·7	4·0	4·0	4·0
OUTPUT CURRENT								
Average current per rectifier leg $I_{F(av)}$		I_{dc}	0·5I_{dc}	0·5I_{dc}	0·33I_{dc}	0·33I_{dc}	0·167I_{dc}	0·167I_{dc}
I_{rms} per rectifier leg	R	1·57I_{dc}	0·785I_{dc}	0·785I_{dc}	0·588I_{dc}	0·577I_{dc}	0·408I_{dc}	0·293I_{dc}
	L		0·707I_{dc}	0·707I_{dc}	0·577I_{dc}	0·577I_{dc}	0·408I_{dc}	0·289I_{dc}
I_{pk} per rectifier leg	R	3·14I_{dc}	1·57I_{dc}	1·57I_{dc}	1·21I_{dc}	1·05I_{dc}	1·05I_{dc}	0·605I_{dc}
	L		I_{dc}	I_{dc}	I_{dc}	I_{dc}	I_{dc}	0·5I_{dc}
TRANSFORMER RATINGS								
Secondary r.m.s. voltage per transformer leg $E_{T(rms)}$		2·22E_{dc}	1·11E_{dc} (to centre-tap)	1·11E_{dc}	0·855E_{dc} (to neutral)	0·428E_{dc}* (to neutral)	0·74E_{dc} (to neutral)	0·855E_{dc} (to star point)
Secondary r.m.s. current per transformer leg $I_{T(rms)}$	R	1·57I_{dc}	0·785I_{dc}	1·11I_{dc}	0·588I_{dc}	0·816I_{dc}*	0·408I_{dc}	0·293I_{dc}
	L		0·707I_{dc}	I_{dc}	0·577I_{dc}	0·816I_{dc}*	0·408I_{dc}	0·289I_{dc}
Secondary volt-amp VA_s	R	3·48$E_{dc}.I_{dc}$	1·74$E_{dc}.I_{dc}$	1·23$E_{dc}.I_{dc}$	1·50$E_{dc}.I_{dc}$	1·05$E_{dc}.I_{dc}$	1·81$E_{dc}.I_{dc}$	1·50$E_{dc}.I_{dc}$
	L		1·57$E_{dc}.I_{dc}$	1·11$E_{dc}.I_{dc}$	1·48$E_{dc}.I_{dc}$	1·05$E_{dc}.I_{dc}$	1·81$E_{dc}.I_{dc}$	1·48$E_{dc}.I_{dc}$
Secondary utility factor U_s	R	0·287	0·574	0·813	0·666	0·95	0·552	0·666
	L		0·636	0·90	0·675	0·95	0·552	0·675
Primary voltage per transformer leg (transformer ratio 1:1)		2·22E_{dc}	1·11E_{dc}	1·11E_{dc}	0·855E_{dc}	0·428E_{dc}	0·74E_{dc}	0·855E_{dc}
Primary current per transformer leg (transformer ratio 1:1)	R	1·57I_{dc}	1·11I_{dc}	1·11I_{dc}	0·588I_{dc}	0·816I_{dc}	0·577I_{dc}	0·408I_{dc}
	L		I_{dc}	I_{dc}	0·471I_{dc}	0·816I_{dc}	0·577I_{dc}	0·408I_{dc}
Primary volt-amp VA_p	R	3·48$E_{dc}.I_{dc}$	1·23$E_{dc}.I_{dc}$	1·23$E_{dc}.I_{dc}$	1·50$E_{dc}.I_{dc}$	1·05$E_{dc}.I_{dc}$	1·28$E_{dc}.I_{dc}$	1·05$E_{dc}.I_{dc}$
	L		1·11$E_{dc}.I_{dc}$	1·11$E_{dc}.I_{dc}$	1·21$E_{dc}.I_{dc}$	1·05$E_{dc}.I_{dc}$	1·28$E_{dc}.I_{dc}$	1·05$E_{dc}.I_{dc}$
Primary utility factor U_p	R	0·287	0·813	0·813	0·666	0·95	0·78	0·95
	L		0·90	0·90	0·827	0·95	0·78	0·95

*For three-phase full-wave bridge a delta-connected secondary can also be used. Then:
r.m.s. voltage per transformer leg = 0·74E_{dc} and r.m.s. current per transformer leg = 0·472I_{dc}

R = resistive load   L = inductive load   f = supply frequency Hz (c/s)

In the calculation of the above circuit performances, the rectifier forward voltage drop and the transformer impedance have been ignored.

The primary volt-amp rating of the transformer does not take primary magnetising current into account.

Firing of Ignitrons by means of Thyristors

H. J. G. M. van Daelen
Philips Development Laboratory, Ignitrons, Eindhoven

This article deals with the design considerations of ignition circuits for ignitrons, incorporating thyristors. After a brief discussion of the ignition mechanism of ignitrons, the anode excitation circuit is dealt with. Several circuits are described in which the voltage appearing across the thyristor is stepped down so as to allow the use of low-voltage thyristors. Subsequently the separate excitation circuit is investigated, the optimum design of which depends greatly on the conditions which the welding machine is intended for.

INTRODUCTION

In order to ignite an ignitron a certain amount of energy must be supplied to its ignitor at the appropriate instant. This energy must be sufficient to initiate an arc discharge between this ignitor electrode and the mercury-pool cathode. A 'cathode hotspot' is then formed, and provided the anode voltage is high enough during the time that this discharge is sustained, the anode will take over the discharge from the ignitor. The main circuit is thus closed.

There are two types of ignition circuit, namely the *anode excitation* circuit and the *separate excitation* circuit.

With *anode excitation* the ignition energy is taken from the anode circuit of the ignitron which is to be ignited. No auxiliary energy source need thus be provided, and ample energy is available to ensure reliable operation. However, with this method of operation the instant of ignition, and hence the phase delay angle, cannot be chosen deliberately since the ignitor voltage must have reached a certain value (> 200V) in order to initiate the discharge.

Because the *separate excitation* circuit is independent of the conditions prevailing in the anode circuit, it can be used at low anode supply voltages, and the firing angle can be varied within wide limits. However, the optimum design is dictated by a number of factors, as will be shown later. An additional advantage of this circuit is that the operation of the thyristors is not endangered by unpredictable phenomena (such as voltage transients) which may occur in the anode circuit.

Before dealing with these two modes of operation and discussing the use of thyristors in the ignition circuit, it will be useful to give a brief explanation of the ignition mechanism of ignitrons.

IGNITION MECHANISM

Ignitrons contain an ignitor made of semiconductor materials (mainly boron carbide) which is so mounted that its tip dips into the mercury pool cathode. The mercury thus forms a meniscus around the rough surface of the ignitor (Fig. 1).

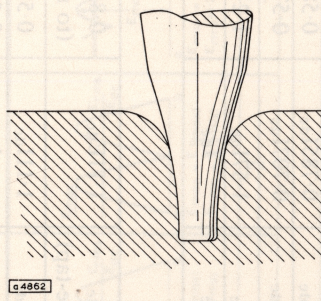

Fig. 1—Ignitor dipping into the mercury-pool cathode

In order to cause field emission of electrons from the mercury pool, a very high electrical field strength must be built up (of the order of 10^5V/cm). The electrons thus liberated must, in addition, encounter a certain minimum local gas pressure, because only in that case will collision ionisation give rise to the formation of sufficient ions to establish the gas discharge. These ions will travel toward the mercury pool cathode, thus surrounding it by a sheath of ions which sustains the field emission.

Once current starts to flow across the ignitor-to-cathode gap it will raise the temperature locally and thus increase the vapour pressure. The higher the rate of rise of the current, the closer will the high-temperature area be confined to the immediate vicinity of the current path where the higher vapour pressure is required; in other words the more adiabatic this process will be. Under these conditions the ignition delay can be very short.

This is illustrated by the curve in Fig. 2 in which the time t required for ignition is plotted against the ignitor current I_{ig}. The slope of the line representing the rate of rise of the current di/dt must in any case be so high that this line intersects the curve to the left of its minimum. If its slope is less than that of the tangent to the right-hand part of the curve, the ignitron will not be ignited, however large the ignitor current may be. The vapour pressure will then have risen excessively before a sufficient field strength has been built up. The discharge is then smothered in the high vapour pressure and no longer maintained.

On the other hand, neither should the rate of rise be too high, since insufficient time would then be available to build up the vapour pressure. The discharge is then likely to be initiated at the place where the least energy happens to be required and not at the required spot, where the distance between ignitor and cathode is smallest. The voltage required to produce the necessary field strength would then have to be very high. Another disadvantage of an excessively high rate of rise of the ignitor current is that electron erosion is apt to reduce the life of the ignitor.

Reprinted from *Electronic Applications*, Vol. 25, No. 4, 1965.

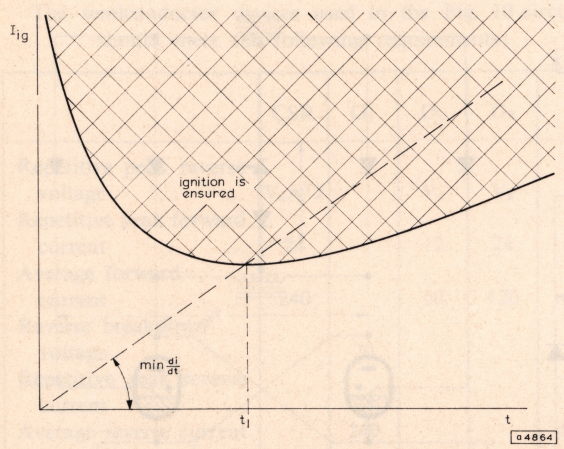

Fig. 2—Typical ignition current characteristic of an ignitron

The ignition energy E which is necessary to ensure ignition of the main discharge depends in turn on the ignition delay, as shown by Fig. 3, in which the shaded area again represents the region within which ignition is ensured. Unfortunately, the minimum of the current characteristic t_i (in Fig. 2) does not coincide with the region where the energy is smallest. In designing the ignition circuit, a choice must therefore be made between a system with which either the ignition current or the energy is a minimum. In the case of anode excitation, where ample energy is available, the former mode of operation is chosen, whereas in the case of separate excitation the latter mode is more economical.

ANODE EXCITATION

Anode excitation is achieved by connecting the ignitor to the anode of the ignitron via a control device comprising a rectifying element and a current-limiting element. With this mode of operation the energy available for initiating the main discharge offers no problem whatsoever, since it is derived from the main circuit. However, if the load is highly inductive, the rate of rise of the current may not be sufficient to ensure ignition.

Apart from its simplicity, this mode of operation offers the advantage that, because the ignitor and the anode circuits are linked, the anode will take over the ignitor discharge automatically and with certainty, once the requirement imposed on the rate of rise of the ignitor current is satisfied. The ignition circuit must obviously be so designed that the voltage drop produced across it exceeds the anode-to-cathode arc voltage.

In the past it was customary to use thyratrons for controlling ignitrons, but preference is now usually given to thyristors, which have a longer life and require no heater supply. However, it should be kept in mind that although thyristors can serve the same purpose as thyratrons, their characteristics are in many respects different, so that the circuit must be adapted accordingly.

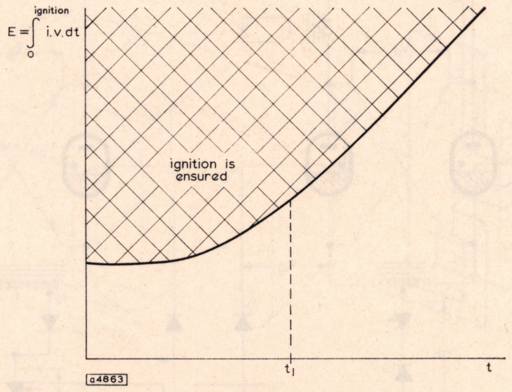

Fig. 3—Typical ignition energy characteristic of an ignitron

Figs. 4 and 5 show two anode excitation circuits equipped with thyristors. In both circuits a voltage source, for example a voltage regulator diode, must be connected in series with each thyristor. This is necessary because the voltage drop across a conducting thyristor is so much smaller than the arc voltage of the ignitron that an excessive current would flow through the thyristor and ignitor during the entire period of conduction of the ignitron.

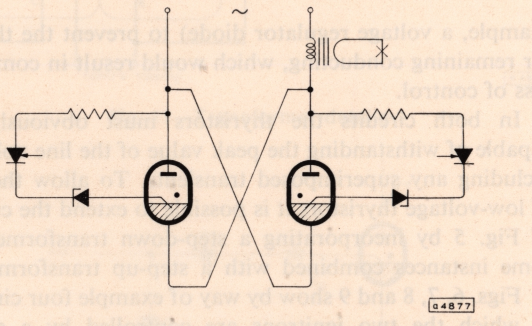

Fig. 4—Anode excitation circuit with two thyristors

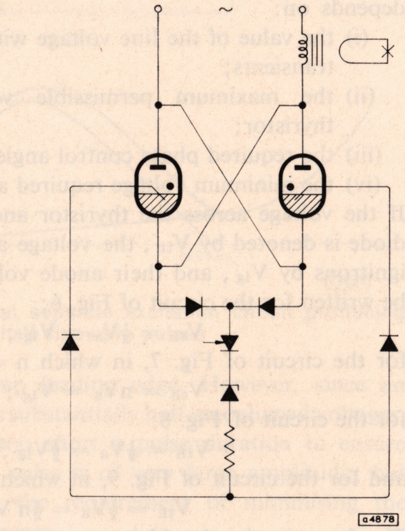

Fig. 5—Anode excitation circuit in which ignition of both ignitrons is controlled by a single thyristor

The circuit in Fig. 5 offers the advantage that both ignitrons are controlled by a single thyristor. In this circuit is is imperative to incorporate an additional device which ensures a current-independent voltage drop (for

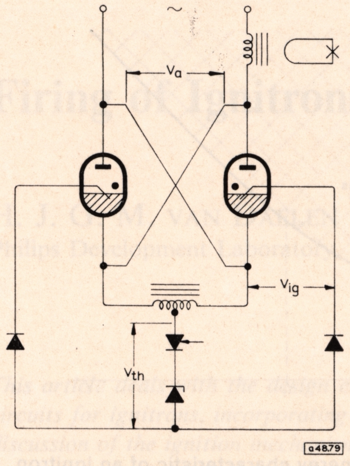

Fig. 6

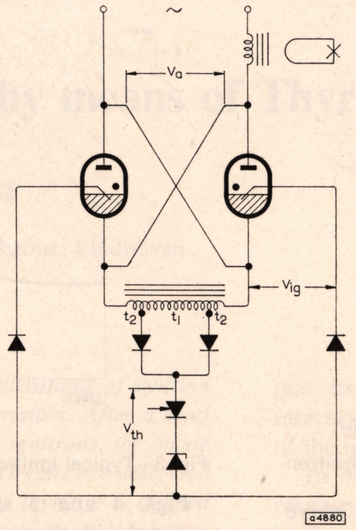

Fig. 7

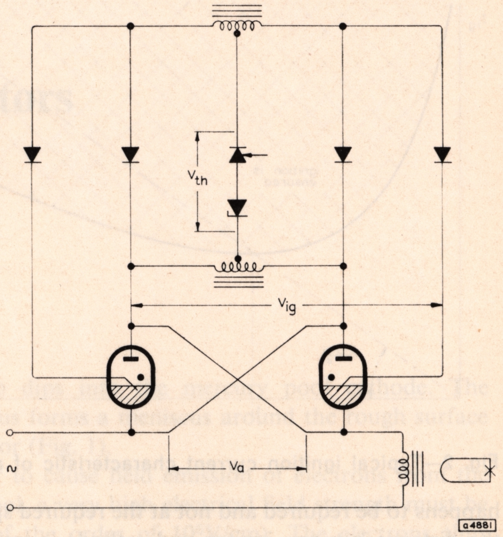

Fig. 8

Figs. 6 to 9—Four anode excitation circuits in which the anode voltage is stepped down to allow the use of low-voltage thyristors

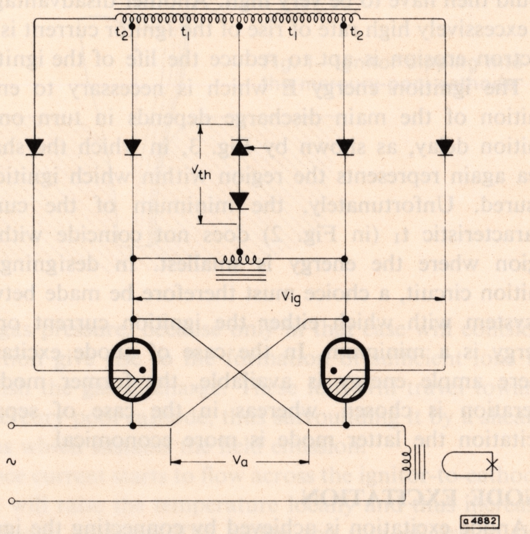

Fig. 9

example, a voltage regulator diode) to prevent the thyristor remaining conducting, which would result in complete loss of control.

In both circuits the thyristors must obviously be capable of withstanding the peak value of the line voltage, including any superimposed transients. To allow the use of low-voltage thyristors it is possible to extend the circuit of Fig. 5 by incorporating a step-down transformer, in some instances combined with a step-up transformer.

Figs. 6, 7, 8 and 9 show by way of example four circuits in which the two ignitrons are controlled by a single thyristor. Which of these circuits is to be preferred depends on:

(i) the value of the line voltage with its superimposed transients;

(ii) the maximum permissible voltage across the thyristor;

(iii) the required phase control angle;

(iv) the minimum voltage required at the ignitor.

If the voltage across the thyristor and voltage regulator diode is denoted by V_{th}, the voltage at the ignitor of the ignitrons by V_{ig}, and their anode voltage by V_a, it can be written for the circuit of Fig. 6:

$$V_{th} = \tfrac{1}{2}V_a = V_{ig}\ ;$$

for the circuit of Fig. 7, in which $n = (t_1+t_2)/(t_1+2t_2)$:

$$V_{th} = nV_a = V_{ig}\ ;$$

for the circuit of Fig. 8:

$$V_{th} = \tfrac{1}{2}V_a = \tfrac{1}{2}V_{ig}\ ;$$

and for the circuit of Fig. 9, in which $n' = 2t_1/(2t_1+t_2)$:

$$V_{th} = \tfrac{1}{2}V_a = \tfrac{1}{2}n'V_{ig}\,.$$

The four circuits should in any case be so designed that the impedance is not unduly increased by the incorporation of the step-down (and step-up) transformer. Fig. 10 gives by way of example a worked-out anode excitation circuit based on the principle shown in Fig. 8. The instantaneous value of the mains voltage must be at least 290V at the moment of ignition. Because of circuit losses the ignitor voltage would otherwise not reach the required value of 200V.

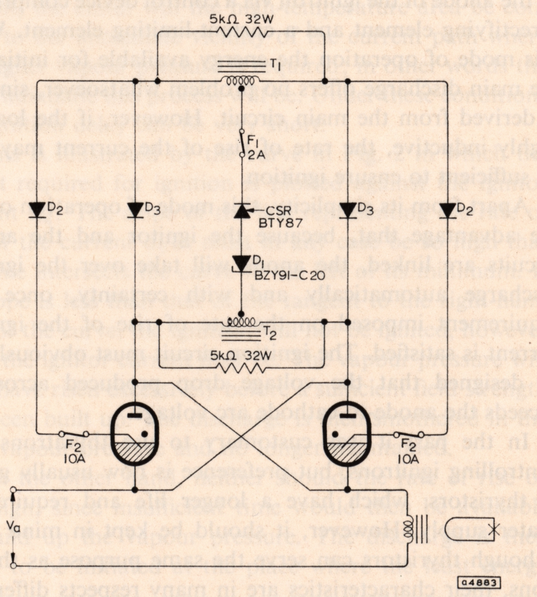

Fig. 10—Practical anode excitation circuit

The semiconductor devices used in the Fig. 10 circuit should meet the following requirements:

	CSR	D_1	D_2	D_3	
Repetitive peak reverse voltage	$V_a/\sqrt{2}$		V_a	V_a	
Repetitive peak forward current	24		12	24	A
Average forward current	240		60	120	mA
Reverse breakdown voltage		20			V
Repetitive peak reverse current		24			A
Average reverse current		240			mA

Autotransformers T_1 and T_2 should differ as little as possible and they should be exactly centre-tapped. Their resistance should be as low as possible ($< 2\Omega$) and their stray inductance should be minimised ($\omega L_s < 0{\cdot}6\Omega$ under short-circuit conditions). The impedance should exceed $2{\cdot}5\text{k}\Omega$ at $V_s = 400\text{V}$. The recommended construction of the transformers is illustrated in Fig. 11. Two double-C cores with a cross-sectional area of 9650mm² are used; the air gap should be less than 5μm. The magnetic flux length is 303mm and the iron weight is 2·1kg per core. The maximum flux density is 1·75Vs/m² (17 500Gs) and the quoted power 255VA at 50Hz. The windings, which surround the adjoined legs, consist of 1·4mm enamelled copper wire. Winding AD is split into two halves, AB and CD, with winding EF sandwiched between.

SEPARATE EXCITATION

With the separate excitation method an auxiliary energy source is discharged into the ignitor-cathode gap at the desired instant. The advantage of this mode of operation is that the ignition energy and the current waveform are independent of the main circuit, so that the ignition circuit can be designed for optimum performance.

Recourse must be had to this mode of operation if the anode voltage is comparatively low and/or the rate of rise of the current in the main circuit is insufficient to use anode excitation. The essential points which have to be considered in designing a separate excitation circuit are:

(i) For reasons of economy, only comparatively little energy can be made available for igniting the ignitrons.

(ii) Once the auxiliary discharge has been established, some time will elapse before the main current has risen to such a value that discharge is taken over. To minimise the risk of omissions (failures to ignite), the ignition circuit must therefore be so designed that the ignitor discharge is maintained for such a period (typically in excess of 200μs) that the main current is given sufficient time to rise to a value of, say, 10 to 12A, at which the discharge is safely taken over by the anode.

The conventional method is to use a simple LC circuit for igniting the ignitron, as shown in Fig. 12. The designer of such a circuit is faced with the following problem. To keep the ignition energy as small as possible, the pulses should have a steep leading edge. However, since an LC circuit produces substantially half-sine shaped voltages, this would imply too short a pulse duration to ensure ignition unless the pulse is of very large amplitude; but this conflicts with the requirement of minimising the required ignition energy.

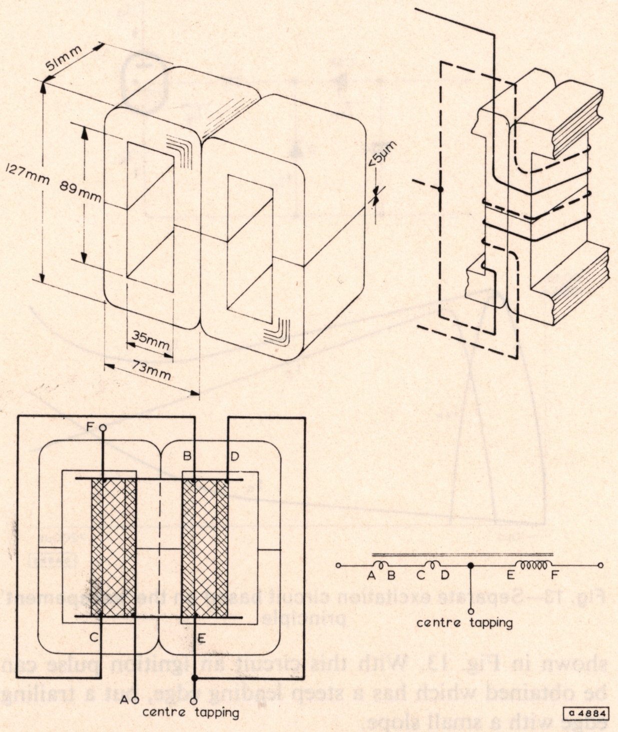

Fig. 11—Transformer details

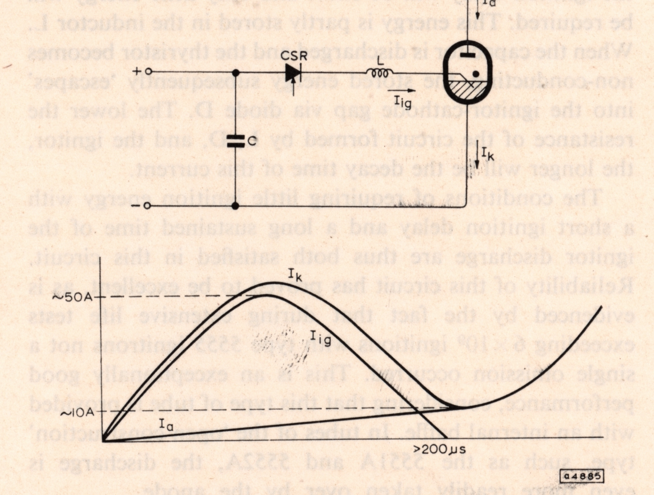

Fig. 12—Conventional separate excitation circuit producing half sinewave pulses

With this type of circuit it is in any case necessary to use very large capacitors, but even then reliability is poor. This is related to the fact that the ignitor current will have started to decrease again before the anode has had the opportunity of taking over the discharge. In this region of rapidly decreasing ignitor current the arc will be unstable and liable to break off.

It is therefore preferable to use the 'escapement circuit'

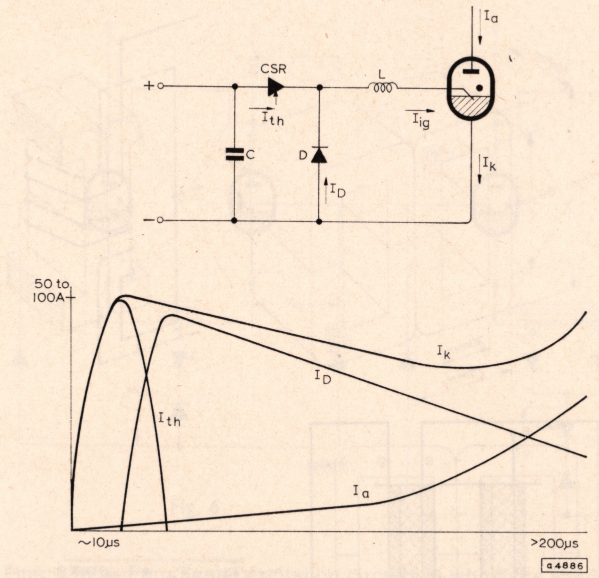

Fig. 13—Separate excitation circuit based on the 'escapement' principle

shown in Fig. 13. With this circuit an ignition pulse can be obtained which has a steep leading edge, but a trailing edge with a small slope.

By using an inductor L of low value (100µH), the ignitor current will have a high rate of rise. As a result, the ignition delay will be short and only little energy will be required. This energy is partly stored in the inductor L. When the capacitor is discharged and the thyristor becomes non-conducting, the stored energy subsequently 'escapes' into the ignitor-cathode gap via diode D. The lower the resistance of the circuit formed by L, D, and the ignitor, the longer will be the decay time of this current.

The conditions of requiring little ignition energy with a short ignition delay and a long sustained time of the ignitor discharge are thus both satisfied in this circuit. Reliability of this circuit has proved to be excellent, as is evidenced by the fact that during extensive life tests exceeding 6×10^9 ignitions with type 5555 ignitrons not a single omission occurred. This is an exceptionally good performance, considering that this type of tube is provided with an internal baffle. In tubes of the 'open construction' type, such as the 5551A and 5552A, the discharge is even more readily taken over by the anode.

In the separate excitation circuit less stringent requirements are imposed on the thyristor than in the anode excitation circuit. Since the supply voltage of the ignition circuit is well-defined and free of transients, there is no risk of the voltage across the thyristor becoming excessive. A further advantage of the separate excitation circuit is that the thyristor is not shunted across the main discharge, so that no current-limiting device is required.

It should be recognised that in the recommended circuit shown in Fig. 13 the supply voltage of the ignition circuit should be at least 600V to obtain a sufficiently high field strength, particularly if the required energy is to be minimised and a short ignition delay is desired. Occasionally, a lower voltage will suffice, but the storage capacitor must then be of much higher value because the required capacitance increases disproportionately as the voltage is reduced. At 650V a capacitor of 2µF will suffice, but at 350V it should have a value of, say, 10µF.

When the ignitron approaches its end-of-life condition and the ignitor characteristics have become poor, the probability of omissions may rise from, say, one per 10^{10} ignitions to one per 10^4 or even to one per 10^3 ignitions at low values of the supply voltage.

The desired reliability will differ from case to case. In seam welds, for example, a single omission will seldom be objectionable, but if spot welds are to be made, an omission will usually be unacceptable. The design of the circuit therefore depends largely on the purpose for which the welding machine is intended. An inexpensive ignition circuit may be quite satisfactory for a seam-welding machine, the more so because the ignitrons are then operated at a high average current and hence at a high duty factor. Under these operating conditions the ignitor characteristics are likely to remain very constant. If, on the other hand, the ignitrons are used for spot-welding purposes under conditions of maximum demand power and a low duty factor, the ignitor characteristics are more apt to deteriorate in time. In designing the ignition circuit, a greater safety margin must therefore be allowed, particularly since the consequences of a single omission may be quite serious.

Figs. 14 and 15 show examples of such ignition circuits which ensure reliable operation both initially and over life. By incorporating an autotransformer which steps up the ignition voltage to a sufficiently high value, a low-voltage thyristor can be used. Provided that the stray inductance of this transformer and its short-circuit resistance are small, the operation of these circuits may be considered identical to that shown in Fig. 13. The circuit of Fig. 15 differs from that shown in Fig. 14 in that the autotransformer is designed to have a stray inductance of 100µH (measured at the secondary), so that the separate inductor of this value can be omitted.

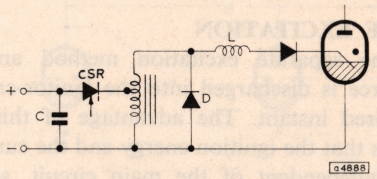

Fig. 14—Circuit similar to that shown in Fig. 13, but with a step-up autotransformer, so that it can be equipped with a low-voltage thyristor

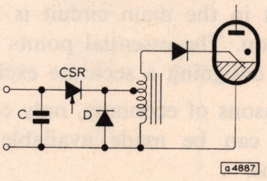

Fig. 15—Circuit equivalent to Fig. 14, but the autotransformer has a stray inductance such that no separate inductor is required